Advances in Colloid and Interface Science 320 (2023) 102983

Contents lists available at ScienceDirect

Advances in Colloid and Interface Science

journal homepage: www.elsevier.com/locate/cis

Historical Perspective

Synthetic and biopolymeric microgels: Review of similarities and difference in behaviour in bulk phases and at interfaces

Daisy Z. Akgonullu [a], Brent S. Murray [a], Simon D. Connell [b], Yuan Fang [c], Bruce Linter [d], Anwesha Sarkar [a,*]

[a] Food Colloids and Bioprocessing Group, School of Food Science and Nutrition, University of Leeds, UK
[b] Molecular and Nanoscale Physics Group, School of Physics and Astronomy, University of Leeds, UK
[c] PepsiCo, Valhalla, New York, NY, USA
[d] PepsiCo International Ltd, Leicester, UK

ARTICLE INFO

Keywords:
Interfacial tension
Pickering stabiliser
Rheology
Viscoelasticity
Microgel particle
Packing

ABSTRACT

This review discusses the current knowledge of interfacial and bulk interactions of biopolymeric microgels in relation to the well-established properties of synthetic microgels for applications as viscosity modifiers and Pickering stabilisers. We present a timeline showing the key milestones in designing microgels and their bulk/interfacial performance. Poly(N-isopropylacrylamide) (pNIPAM) microgels have remained as the protagonist in the synthetic microgel domain whilst proteins or polysaccharides have been primarily used to fabricate biopolymeric microgels. Bulk properties of microgel dispersions are dominated by the volume fraction (ϕ) of the microgel particles, but ϕ is difficult to pinpoint, as addressed by many theoretical models. By evaluating recent experimental studies over the last five years, we find an increasing focus on the analysis of microgel elasticity as a key parameter in modulating their packing at the interfaces, within the provinces of both synthetic and biopolymeric systems. Production methods and physiochemical factors shown to influence microgel swelling in the aqueous phase can have a significant impact on their bulk as well as interfacial performance. Compared to synthetic microgels, biopolymer microgels show a greater tendency for polydispersity and aggregation and do not appear to have a core-corona structure. Comprehensive studies of biopolymeric microgels are still lacking, for example, to accurately determine their inter- and intra- particle interactions, whilst a wider variety of techniques need to be applied in order to allow comparisons to real systems of practical usage.

1. Introduction

Microgels (or also commonly known as microgel particles) are defined as discrete units of a network of cross-linked solvated polymers ranging in radii from hundreds of nanometres to tens of microns [1,2]. Typically, microgels consist of a closely crosslinked core which, as it extends to the periphery, becomes looser - commonly described as a fuzzy exterior of dangling chains [1]. Due to the combination of their gelled structure and polymeric composition, microgels possess unique deformability, leading to viscoelastic performance in bulk media. Whilst the solvent phase of microgels provides them with the ability to swell, the quantity of polymer incorporated in them allows for microgel elasticity to be tuned so that the final particle deformability can be altered [3,4].

Besides bulk properties, microgel particles can adsorb at interfaces with a high desorption energy, thus providing high stability to coalescence of emulsions via a Pickering-like stabilization from soft particles, that has also been termed as “Mickering stabilization” [5–7]. At the same time, microgels can interpenetrate and/or flatten at fluid-fluid interfaces, providing unique interfacial features compared to the case of a typical solid particle adsorbing at the interface [4]. It has been realised that microgels alter their behaviour in the continuous phase compared to when they are interacting with an interface (solid-fluid, fluid-fluid) [8,9]. In bulk solution/dispersion, microgels appear swollen; their chains are solvated and can entangle if present in close proximity. However, when adsorbed to an interface microgels are thought to develop a ‘fried egg’ like structure due to their outer layers flattening out, whereas the denser packing of the centre of the microgel maintains a greater height [10].

There has been much development of synthetic microgels, most

* Corresponding author.
E-mail address: A.Sarkar@leeds.ac.uk (A. Sarkar).

https://doi.org/10.1016/j.cis.2023.102983
Received in revised form 12 August 2023;
Available online 15 August 2023

notably extensive research in the last couple of decades on the production and properties of poly(N-isopropylacrylamide (pNIPAM) microgels. Details of pNIPAM microgel synthesis were first published in 1986 [11] and the principles behind their properties have been investigated in many areas, including nanolithography [12], sensors [13], water management [14], pesticide release [15], drilling fluids [16] and coatings [17]. These potential applications exploit the thermo-responsive nature of the pNIPAM polymer, plus the ability to modify these characteristics by varying the precursors and co-monomers, leading to many variations. Examples include responsiveness to pH [18], ionic strength [19], sugar [20], light [22,23] and antimicrobial activity [24]. Although they have shown impressive versatility, pNIPAM microgels do pose a risk of cytotoxicity [25], thus their application for biotechnological, biomedical and food purposes is probably not feasible. Other, biocompatible synthetic microgels have been constructed based on ethylene glycol (EG) [21,26] and vinyl caprolactam (VCL) [27]. However, there is still a clear need for biodegradable microgels based on increasing needs of sustainability to reduce their possible environmental impact [28], and to enable their large-scale manufacture and use within food and drink [29,30], for example.

Microgels of biopolymer origin have a strong potential for products with the capacity for encapsulation and controlled release, which could help to tackle a range of formulation challenges within food, pharmaceutical, agrochemical, biotechnological and allied industries - where biocompatibility and sustainability are currently key issues [31–33]. Although lipidic microgels do exist [34–37], non-lipidic microgels fabricated using proteins and polysaccharides may be advantageous as these are biodegradable [30], food-grade [38] and easily available [39], plus they might also enable exploitation of current agricultural and food production waste streams [40,41]. Biopolymeric microgels can be produced using a variety of methods [32,42,43] and have equally been shown to act as Pickering emulsion stabilisers [44], foaming agents [45] and modifiers of viscosity in the continuum [46]. However, a full understanding of their mode of action and optimization of their stabilising characteristics still remains to be achieved. As research in this area progresses to provide information on their detailed behaviour at real fluid interfaces [47], key to all these studies is the need for a better understanding of the microgel particle-particle interactions that occur at large to short length-scales.

This review therefore aims to present an overview of microgel research with a focus on the last 5 years, to summarise the current knowledge of their bulk and interfacial properties and how this may be applied to enable future progress in their fabrication from biopolymeric sources. It is acknowledged that the term 'microgel' is, in some cases, used interchangeably with other terms such as: 'nanogel', which has recently been defined as microgels with sizes below 1 μm [4]; 'hydrogel', which may be up to millimetres in diameter [2]; 'fluid gel', particles gelled under shear and with a tendency for a less structured, 'tadpole' shape [48]. We have thus limited our scope to particles which meet the size requirement of 100 nm to 10 μm, in order to consider behaviour specific to this size range in dispersions and at interfaces. We will briefly explain the characteristics of the more well-established synthetic microgels first, followed by a detailed discussion of the less well studied biopolymeric microgels, to evaluate how previous studies and theoretical models of synthetic microgels might inform the future design of bespoke biopolymeric microgels for more specific needs. We will mainly focus on bulk and interfacial performance reported within experimental studies, whilst readers may refer to other previous reviews of biopolymeric and synthetic microgel particles, covering their fabrication and potential applications within foams and emulsions [7,32,33,49–52] as well as recent simulation studies [8,53–55].

2. Timeline of key milestones of microgel synthesis and properties

Fig. 1 highlights key milestones in the understanding of microgels. The first report of microgel synthesis was in 1935 [56], as part of Staudinger and Husemann's pioneering studies of polymer science. However, the terminology of 'microgel' appears to originate in 1949, defined by Baker as a 'new macromolecule' [57]. Following this, studies of the viscosity of microgel dispersions emerged, with proposals of microgel osmotic de-swelling behaviour [58] and their capacity to act as thickeners in solution [59]. Towards the end of the 1990s, the role of microgel 'dangling ends' was considered in modelling of their interactions in concentrated solutions [60], which clearly emphasised their difference from hard sphere behaviour. These milestones [58–60] explored microgel behaviour in a continuum but the interfacial characteristics of microgels were not greatly focused on until ca. 2000 onwards. In 1999, Zhang and Pelton [61], observed the surface activity of pNIPAM microgels at the air-water interface and this is thought to be the first report of microgel facilitated reduction in surface tension. Since this finding, there have been a series of proposed microgel applications

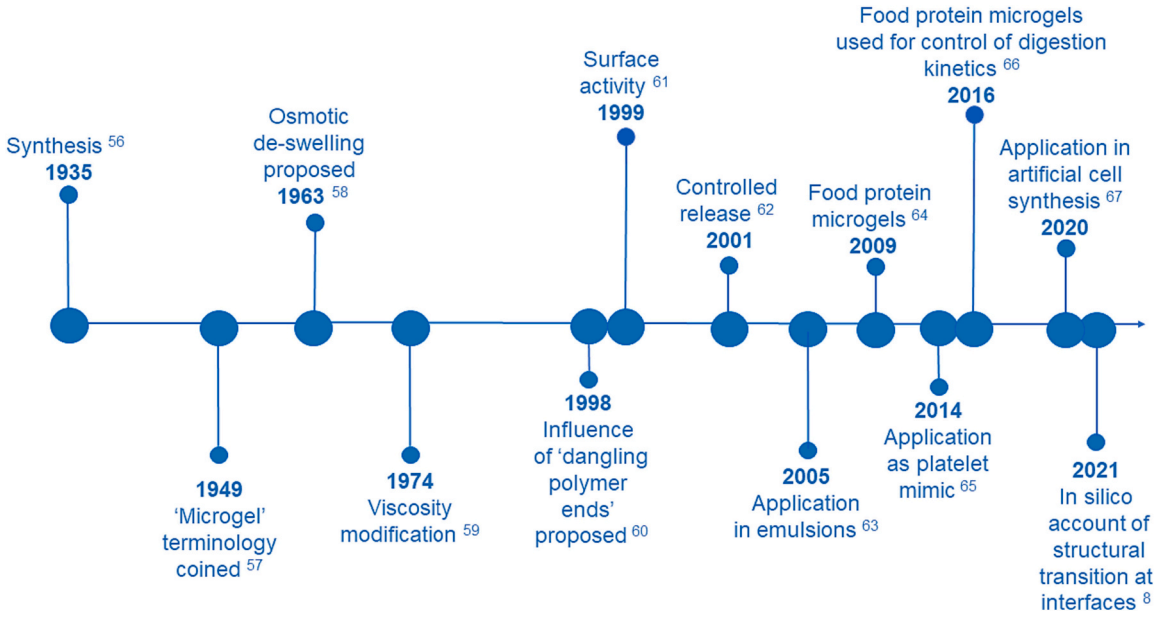

Fig. 1. Timeline displaying milestones in the understanding of microgels and their application.

[62–67], with increasing emphasis on the ability to tune microgel deformability [8,68] as a unique advantage in the formulation of controlled release systems, cellular update and bio-mimetic design (see Fig. 1).

3. Bulk properties of microgels

Recent literature has shown an increase in investigations of the rheology of microgel dispersions, with synthetic microgels dominating the field with 70% of papers, and biopolymer systems representing 30% (Fig. 2). Studies of synthetic microgels primarily focus on pNIPAM microgels due to the ease of their production via polymerisation and adaptation of their responsiveness [6], whilst other synthetic systems tend to be based on polyacrylic acid. Biopolymeric microgels are typically produced through thermal gelation, whilst pH and enzymatic triggered means are being increasingly explored (Table 1). These methods yield microgel particles by utilising the diverse physiochemical and conformational properties of biopolymers such as their charge distribution, molecular weight, chain lengths and denaturation temperature to promote polymer gelation [32].

For synthetic microgels, the temperature responsiveness of pNIPAM has been a key manipulation factor to achieve rheological modulation (Fig. 2). However, for biopolymeric microgels, charge-mediated interactions dominate because of the poly-ionic nature of polar proteins and some polysaccharides, with pH being the main factor tested for synthesizing microgels for rheological modification. In this section, we will discuss the recent trends in microgel behaviour within the continuum and analyse how findings from synthetic microgel systems may be applied to those of biopolymer origin. Firstly, we describe the behaviour of microgels with increased packing, before considering phenomenological models of microgel suspensions and the role of physiochemical characteristics affecting microgel flow.

3.1. Role of particle deformation during flow

Microgels have a strong influence on the flow of suspensions that contain them, however their exact flow behaviour is difficult to quantify due to their deformable structure – often they aggregate or collapse as a result of the flow, which in turn alters the rheological properties, which is then often dependent on the shear history. Deformation of microgels within the continuum has been directly observed using confocal imaging [69] and stochastic optical reconstruction microscopy (STORM) [70,71], and has been reported to occur in a number of different forms:

- De-swelling: solvent expulsion, which alters the particle's volume
- Compression: flattening of particles due to confinement from their surroundings e.g., promoted by shear, strain, gap size *e.g.* in narrow outlet
- Faceting: modification of microgel edges, thus changing the sphericity/ roughness of the particle
- Interpenetration (interdigitation): fusing of microgels via their exterior polymer chains

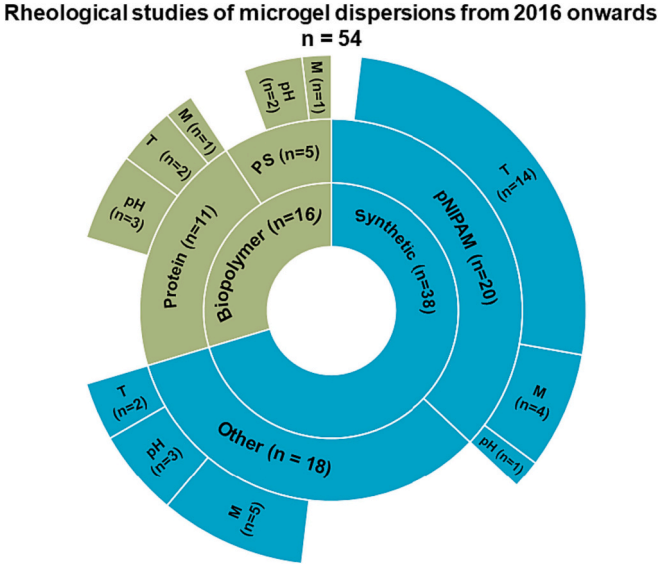

Fig. 2. Recent studies ($n = 54$) that have surfaced since 2016 involving rheological characterization of microgel dispersions, organised by biopolymer (where PS: polysaccharide) or synthetic microgels with various types of physiochemical variation (T: temperature, M: ionic strength and pH).

Investigations of the volume occupied by microgels in a dispersion (volume fraction, ϕ) have been conducted with the aim of understanding the precise nature and influence of particle packing on rheological properties [4]. However, due to the above possible mechanisms of deformation, it is difficult to determine an exact volume fraction for these kind of systems, unlike rigid spheres. Therefore, measurements of volume fraction are often referred to as effective or generalised volume fractions (ϕ_{eff}) since these values are inferred [4,72]. Recent studies have utilised small angle X-ray scattering (SAXS) and small angle neutron scattering (SANS) with contrast variation to obtain values of 'real' microgel volume fractions in solution [73] for synthetic microgels. However, for biopolymeric microgel particles this is further complicated by a high degree of polydispersity in microgel size [74] and this is often calculated indirectly from the mass (density and therefore volume) of the biopolymer gel or solution used in fabricating the microgels [46,75,76].

Frequently, the viscosity and moduli of synthetic microgels are plotted against ϕ (or concentration) and despite variations in the particle size and synthesis methods of these systems, with increasing concentration the emergence of typical regimes can be observed, as the dispersion transitions from a dilute liquid to a viscoelastic solid. These regimes deviate from the behaviour of model rigid spheres, as observed for synthetic microgels fabricated using pNIPAM [4,71,77–79], polyacrylamide [80,81], derivatives of polyethylene glycol (PEG) [82] or polyacrylic acid [83]. Often $\phi_{eff} > 1$ for microgels due to their deswelling, deformation, or interpenetration, which of course is impossible for true hard spheres [84]. Fig. 3 provides a schematic representation of potential interactions in relation to commonly used models for aforementioned synthetic microgels published in the recent literature. Although such regimes might also hold well for biopolymeric microgels [74], limited data in the literature makes such conclusions difficult.

3.1.1. Dilute Regime

Generally, microgel dispersions tend to show a plateau in viscosity at low shear (zero shear viscosity, η_0), followed by a region of shear-thinning behaviour, which leads to a second plateau at high shear (infinite shear viscosity, η_∞). At low concentrations [74,80], microgels such as those made from polyacrylamide are separated and not in direct contact with each other, thus their behaviour is determined by external shear forces and there is little extra resistance to flow over that of the continuous phase. Thus, as shown in Fig. 3a, this regime shows low values of relative viscosity (i.e., the ratio of viscosity of the dispersed particles to the continuum) (η_r). Storage and loss moduli (G', G'', *respectively*) are such that $G'' > G'$,throughout, i.e., liquid-like behaviour dominates. For example, Scotti et al. [79] reported values of η_r in the region of 10^0–10^1 for pNIPAM microgel systems up to approximately $\phi_{eff} = 0.4$.

Nevertheless, such 'dilute' dispersions can show non-Newtonian behaviour when subjected to high shear rates, because these synthetic microgels synthetized from polyacrylamide, PEG derivatives, pNIPAM + polyacrylic acid may alter their orientation and shape with respect to the direction of flow, due to compression by the shear forces, which can

Table 1
Suite of techniques used for interfacial characterization of biopolymer microgels at liquid-liquid interface.

Bio-polymeric Microgel Type	Biopolymeric Microgel Production	D_H* (nm)	Probing interface						Ref.
			IFT	Langmuir-Blodgett	Dilatational Modulus	AFM	Electron Microscopy	Other	
Agar, gellan gum and curdlan	Top down – Thermal crosslinking and shearing cf. Bottom up – Controlled stirring during thermal crosslinking (chemical for gellan gum)	6800, 86, 4000	✔	–	–	–	✔ Cyro-SEM	ζ-potential, CLSM, Bulk shear viscosity, H_o	[167]
(κ-) Carrageenan	Top down – pH adjustment, thermal crosslinking, and shearing	213	✔	–	–	–	✔ FE-SEM	ζ-potential, CLSM, CA, Interfacial shear moduli, FTIR, Optical microscopy	[172]
Chitosan	Top down - Ionic crosslinking and ultrasound	615	✔	–	✔	✔	–	ζ-potential, FTIR, CLSM	[125]
Egg white protein	Top down - Thermal crosslinking and shearing	359	–	–	–	–	✔ Cyro-SEM	Interfacial shear viscosity, CLSM	[45]
Myofibrillar protein	Top down – Thermal crosslinking and shearing	100	–	–	–	✔	–	ζ-potential, CA, H_o	[178]
Pectin	Top down - Acid gelation and shearing	79	✔	–	–	–	–	–	[174]
Soy protein	Top down – Enzymatic crosslinking and shearing	100 **	✔	–	✔	–	✔ FE-SEM	ζ-potential, CLSM, CA, H_o,	[177]
Whey protein [179] (*β-lactoglobulin* [168,173])	Bottom up - Acid gelation followed by pH adjustment, heating, ultrafiltration [179] or thermal crosslinking, and centrifugation [168,173]	90 [179], 100 ** [173], 207 [168]	✔	✔	✔ [168]	✔ [168]	✔ TEM [179]	ζ -potential [179], QCM-D [173], FTIR [173], EM [173]	[168,173,179]
Whey protein	Bottom up - Water-in-oil emulsion, followed by thermal crosslinking, and freeze-drying [176], ionic crosslinking, and freeze-drying [169] or thermal crosslinking, centrifugation, homogenisation [124]	220 ** [169], 400 [124], 990 [176]	✔ [169,176]	✔ [169]	✔ [169,176]	✔[165]	✔ SEM[119, 165]	ζ-potential, Interfacial shear moduli [169], Ellipsometry [176], Optical microscopy [176], Bulk shear viscosity [124]	[124,169,176]
Whey protein [171] (*β-lactoglobulin* [170])	Top down - Thermal crosslinking, spray dried, rehydrated, shearing [171], or Acid gelation, thermal crosslinking, and shearing [170]	100 [170], 248 [171]	✔ [170]	✔ [170]	✔ [170]	✔ [170,171]	–	QCM-D[162], FTIR[162], EM[162], Optical microscopy [170], BAM [170]	[170,171]

AFM: Atomic force microscopy, BAM: Brewster angle microscopy, CA: Three phase contact angle, CLSM: Confocal light scanning microscopy, EM: Electrophoretic mobility, FE-SEM: Field emission scanning electron microscopy, FTIR: Fourier transform infra-red spectroscopy, H_o: Surface hydrophobicity, IFT: Interfacial tension, QCM-D: Quartz crystal microbalance with dissipation, SEM: Scanning electron microscopy, TEM: transmission electron microscopy, ζ-potential: Zeta Potential.

* Hydrodynamic diameter quoted as smallest average size stated from light scattering analysis, with the exception of AFM measurement [170] and Coulter sizing measurement for agar and curdlan microgels [167].

** Hydrodynamic diameter inferred from graph.

lower the apparent viscosity [81–83,85].

3.1.2. Glassy Regime

In the second regime (Fig. 3b), dispersions become increasingly viscous with increase in ϕ_{eff}. Firstly, the dispersion passes through a glass transition (at $\phi_{eff} = \phi_g$). For rigid spheres, it has been reported that $\phi_g = 0.58$, but due to the softness of microgels, ϕ_g is higher [80]. Higher levels of polydispersity in size and irregularly shaped particles have also been suggested as contributors to reducing the ϕ_{eff} and ϕ_g at which these transitions occur [74,84].

Within the glassy regime, particles are considered to be in a state of dynamic arrest [86]. As the system becomes more densely packed it can develop a yield stress, i.e., above this stress, the structure collapses and starts to flow [77–80,83]. Particles can be imagined as becoming 'caged' by their neighbouring particles as the ϕ of the particles increases and thus the free motion of individual particles is prevented, and so solid-like behaviour emerges and the viscosity increases enormously (see Fig. 3b). Nevertheless, G' and G'' have still been observed to show frequency dependence, meaning that the system is still only a weak gel and can rearrange and relax within the experimental time scale.

As the microgel concentration increases even further, the suspension reaches the ϕ_{eff} of random close packing (ϕ_{rcp}) which can also be referred to as the 'jamming point'. For perfect, monodisperse hard spheres $\phi_{rcp} = 0.64$ [48]. However, for soft microgels their deformability again allows for greater levels of ϕ_{rcp} [75]. Typically, at ϕ_{rcp} suspensions of hard spheres display a divergence in η_r, where there is a swift increase

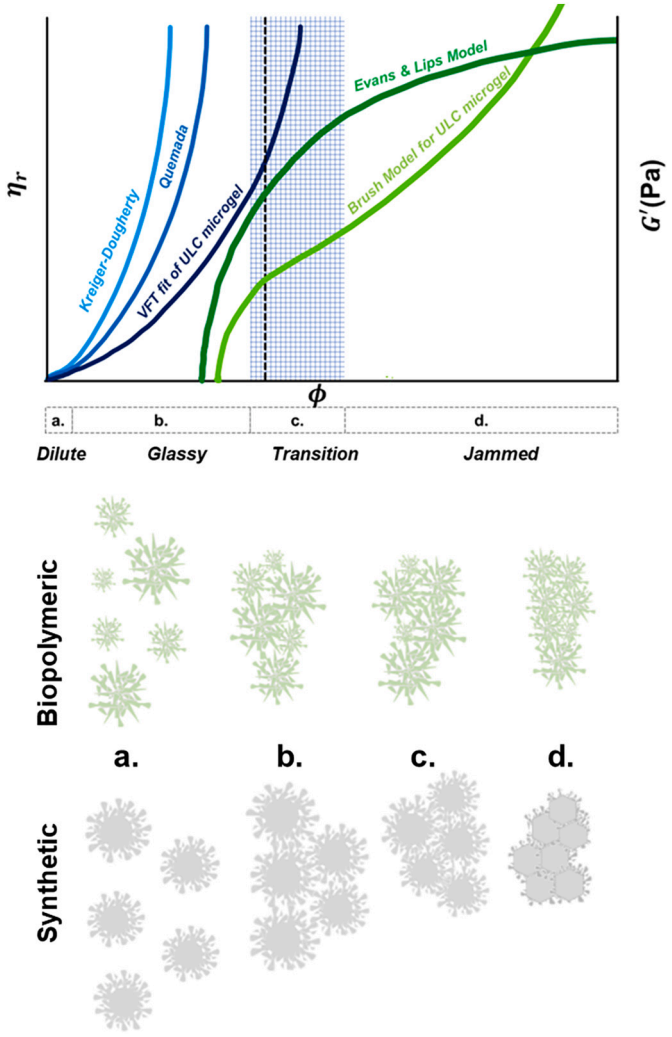

Fig. 3. Schematic illustration of rheological behaviour of microgels showing the relative viscosity of microgels to the continuum (η_r) within four commonly observed regimes with increasing volume fraction, and corresponding models to explain such behaviour. The black dashed line indicates the position of $\phi = 1$, whilst the cross-hatched blue region illustrates the potential transition region from liquid to solid-like behaviour. Reports of models used in recent studies in left-to-right are as follows: Kreiger-Dougherty behaviour [82], Quemada [82,90,91], Vogel-Fulcher-Tramman (VFT), ultra-low crosslinked (ULC) microgel [79], Evans & Lips model [74] and the Brush model [71,79]. The cartoon below the graph indicates the corresponding hypothetical structure of the dispersions, for biopolymeric (top, green) and synthetic (bottom, grey) microgels. (For interpretation of the references to colour in this figure legend, the reader is referred to the web version of this article.)

in viscosity (in theory to an infinite value) as the system becomes tightly packed and flow ceases [48] - see Fig. 3b. For hard sphere systems this represents their limit in random packing [48,79]. For microgel systems this η_r divergence has been reported for much higher values of ϕ_{eff}, such as $\phi_{eff} = 0.93$ for pNIPAM microgels with 5 mol% crosslinker [87], $\phi_{eff} = 0.71$ with use of 1 mol% crosslinker [79] and $\phi_{eff} = 1.45$ for pNIPAM synthesised without crosslinker [79].

For microgel suspensions beyond their respective ϕ_{rcp}, it has been proposed that the peripheral dangling chains forming the corona are compressed [71]. This has been associated with significant increases in G' in pNIPAM microgel systems, for example values of ϕ_{eff} from 0.78 to 1.28 giving an increase in G' by three orders of magnitude [71].

3.1.3. Transition Regime

After an initial rapid increase in G' in the glassy regime, it is believed that a transition in microgel suspension behaviour occurs (Fig. 3c). Above $\phi_{eff} \approx 0.87$ [71], Conley et al. reported the emergence of a regime displaying a slower, linear G' increase as the microgel system became increasingly 'overpacked' and interstitial spaces were gradually reduced. This rheological behaviour was certainly observed for $\phi_{eff} > 1$ in pNIPAM systems [71,83], and attributed to the development of contacts between adjacent microgel cores [71]. Due to the softness of microgel cores, this interaction is suggested to progressively dominate microgel suspension rheology, as ϕ_{eff} increases and external polymer chains are compressed onto the centres of the microgels [71].

Conversely, Shewan et al. [74] reported a viscoelastic fluid region in their study of biopolymeric agar microgels, which was described as a transition prior to the emergence of elastic solid-like behaviour. This was suggested to be at higher ϕ_{eff} than ϕ_{rcp} and was characterized as the point where $G' = G''$ at a constant frequency [74]. It was acknowledged that the length of this transition would be dependent on the exact type of system, with emphasis on the need for investigation of the effects of particle modulus and polydispersity [74].

The means of interpretating the possible transitions into solid-like behaviour are not always clear [78]. Several studies have also calculated a boundary between glass and jammed regimes using the shear stress of a microgel suspension normalised by the stress created by thermal fluctuations [79,83,88]. This normalised shear stress can then be plotted against the Péclet number of the microgels, the ratio of the characteristic flow time to the Brownian diffusion time of the microgels [46]. It has been suggested that the system becomes jammed above a normalised shear stress of 12.5 [79,83,88]. Solid-like behaviour within a jammed regime is considered as an athermal region, where Brownian motion is negligible [79,84]. Therefore, rather than being determined by thermal fluctuations, the internal energy of the system is dictated by physical attributes and the extent of microgel softness, i.e., the individual particle modulus. Inter-particle friction has also been postulated to show an increasing impact [74,84].

3.1.4. Jammed Regime

Following the transition region, growth in the yield stress values tends to slow down with further increase in packing, in some cases the yield stress appearing to plateau [78–80,83]. Here, microgels are viewed as completely trapped by their neighbours, whose elastic energy preserves microgel positioning when the system is subjected to shear and strain, preventing displacement over the observed rheological timescale. Thus $G' > G''$ and both moduli show frequency-independence, *i.e.*, the system shows 'true' solid-like behaviour and this regime is usually referred to as the 'jammed regime' [77,79].

As solid behaviour dominates, the close proximity of adjacent microgels enables them to entangle which can facilitate further deformation, such as the interpenetration of microgel cores as visualised by Conley et al. [71] (see Fig. 3d). This steric confinement may provide greater routes for dissipation and lead to significant changes in the loss modulus (G'') at high packing densities [71]. These changes in G'' could also originate from the formation of facets on microgel surfaces. Faceting has been claimed to result in a net repulsive force and a net drag force, originating from either elastic forces or elastohydrodynamic forces, respectively, at points of particle-particle contact [80]. Faceting has been attributed to polyacrylic acid microgels in transforming into a polygonal shape [89] (see Fig. 3d). Such deformations have been observed in synthetic pNIPAM microgels [69], although this study required use of large microgels to enable their examination via confocal microscopy and use of a dialysis membrane and equilibration against an osmolyte to facilitate homogenous osmotic compression. Thus, further work is needed to fully understand this mechanism under more normal conditions for submicron microgel suspensions. At the same time, since synthetic microgels show greater sphericity than biopolymer

counterparts [84], faceting during jamming might not be as apparent for microgels of biopolymeric origin. Also, it should be remembered that the extent of particle interpenetration will be controlled to some extent by the charge on the polymer chains at the surface [4].

Beyond $\phi > 1.9$, it has been suggested that synthetic microgel systems become 'saturated' since their packing is now homogeneous [71] and osmotic deswelling is negligible due to an even distribution of microgel polymer counterions [80]. Authors have therefore proposed an additional regime of a 'dense glass' [80] or 'dense overpacked state' [71]. It has been suggested that only isotropic compression may act a potential route for further size reduction [71], since it is thought that microgels may reduce their size to cater for steric constraints [80]. Within synthetic microgel studies, it has been suggested that the peripheral corona collapses onto the core, creating a denser core [71] whose size reduces until the point of saturation is reached [78]. At this final packing density, one might expect to see a plateau in values of viscosity and $G^{'}$, but in practice these states are extremely difficult to reach experimentally.

As shown in Fig. 3, these regimes are associated with various mathematical models that aim to predict rheological behaviour: the commonly used models are discussed below.

3.2. Modelling flow behaviour from hard sphere to soft microgels

In this section we summarise the models that have been used to describe the rheological behaviour based on a range of influencing parameters such as volume fraction (ϕ), shear rate ($\dot{\gamma}$) and architecture of the microgels. We also pinpoint where such models do not hold well particularly for biopolymeric microgels.

3.2.1. Volume fraction

The Einstein-Batchelor eq. (1) [92,93] was developed as an extension to the original equation due to Einstein [94] to model Brownian hard spheres. To include the role of hydrodynamic effects and Brownian motion, Batchelor [92] added a quadratic term with the coefficient of 6.2, although this estimate has more recently more been updated to 5.9 [93] and is the value now most commonly used.

$$\eta_r = 1 + 2.5\phi + 5.9\phi^2 \tag{1}$$

The Einstein-Batchelor equation can be utilised to analyse the behaviour of dilute suspensions of both synthetic and biopolymeric microgels - see regime 1 (Fig. 3a) [79,80,84]. At higher ϕ, however, multi-body hydrodynamic interactions are not taken into account fully and the equation fails to predict η_r accurately even for monodisperse hard spheres. More importantly for microgels, the role of de-swelling is not considered [80]. Furthermore, since eq. 1 assumes perfect spheres, this introduces further deviation from real behaviour. There are corrections that can be applied that take into account the aspect ratio of other monodisperse shapes (ellipsoids, etc.), Péclet number [95] and also polydispersity, but the actual variation of the shapes and sizes of biopolymer-based microgels cannot be taken into account fully [74,84].

The Quemada equation [96] (eq. 2) and Krieger-Dougherty equation [97] (eq. 3) are phenomenological equations that were developed to describe hard sphere behaviour. As shown, eq. 3 uses the intrinsic viscosity, i.e., a value of 2.5 for rigid spheres [94]. However, they incorporate a maximum volume fraction term, ϕ_m, to take into account particle packing: at ϕ_m η_r diverges to infinity, to represent how solid-like behaviour starts to dominate as the system becomes tightly packed (see Fig. 3b). This term has been modified within the Quemada equation to better fit biopolymer microgel systems produced in several recent studies [74,90,91].

$$\eta_r = \left(1 - \frac{\phi}{\phi_m}\right)^{-2} \tag{2}$$

$$\eta_r = \left(1 - \frac{\phi}{\phi_m}\right)^{-[2.5]\phi_m} \tag{3}$$

Shewan et al. [74,90] studied microgel systems of agarose (a biopolymer from seaweed) and found an improved fit when equating ϕ_m with a value of ϕ_{rcp} obtained using particle size distribution measurements and the Farr and Groot model [98]. Meanwhile, Roullet et al. [91] modified the ϕ_m term within eq. 2 to be a function of microgel concentration to fit the behaviour of suspensions of sodium caseinate micelles, which to some extent resemble microgels. This was shown to give a better fit to behaviour at higher concentrations, reflecting the inverse relationship between particle softness and concentration and thus the potential influence of micelle deformation was considered [91].

The viscosity of concentrated microgel suspensions can fit well to the Vogel-Fulcher-Tramman (VFT) model, shown in eq. 4 [4,72,79,83], which captures the more gradual increase in viscosity associated with softer particles, such as synthetic ultra-low crosslinked (ULC) particles [79] (see Fig. 3a - c). Eq. 4 has an exponential term related to both ϕ and ϕ_g, where the latter represents the ϕ at which η_r diverges at a glass transition, whilst A is a constant that aims to include the growth of ϕ as the system approaches this divergence, by analogy to temperature in molecular glass formers [79,99].

$$\eta_r = e^{\left(\frac{A\phi}{\phi_g - \phi}\right)} \tag{4}$$

3.2.2. Shear rate ($\dot{\gamma}$)

Both synthetic and biopolymeric microgel suspensions have been observed to show strong shear thinning behaviour due to their ability to deform and align with shear force [85,100]. At low $\dot{\gamma}$ the presence of intermolecular bonds between the particles can provide resistance to and/or deformation in flow [101], whilst greater shear forces (e.g., $\dot{\gamma} \geq 10^2\ s^{-1}$) may disrupt weak interactions of polymer entanglements (e.g., ionic, hydrogen bonds) between the particles [100,102].

It is commonly found that power law models such as the Cross model (eq. 5) can be used to describe the rheological behaviour of systems at dilute or intermediate concentrations [83,103]. Most systems show shear thinning and the Cross model describes the viscosity decrease with increasing shear rate in terms of $\dot{\gamma}_c$, a critical $\dot{\gamma}$ where η is half way between the upper and lower limiting values of η, η_0 and η_∞, and h is a shear thinning exponent [79,84].

$$\eta = \eta_\infty + \frac{\eta_0 - \eta_\infty}{1 + \left(\frac{\dot{\gamma}}{\dot{\gamma}_c}\right)^h} \tag{5}$$

Thus, this model relies on clearly defined plateaus before and after the reduction in η (shear thinning region) as described above for dilute suspensions [79,83]. However, many studies have found it difficult to fit biopolymer microgel systems to this model due to technical limitations preventing access to sufficiently high $\dot{\gamma}$ in order to determine η_∞ [75,104]. Some fits have been observed in whey protein microgels [46], but in some cases only for very soft microgels [84]. The Carreau-Yasuda model (eq. 6) has also been used and includes an additional fit parameter to the Cross model [80,83]. This additional term (see below) includes the longest relaxation time (τ_0), signifying the start of shear-thinning behaviour, whilst a and b are fitting parameters [80] to model stress (σ) as a function of ($\dot{\gamma}$).

$$\sigma(\dot{\gamma}) = \dot{\gamma}\left[\eta_\infty + (\eta_0 - \eta_\infty)\left(1 + (\tau_0\dot{\gamma})^a\right)^b\right] \tag{6}$$

At higher concentrations, when microgel systems are thought to be above ϕ_{rcp}, Fig. 3b - c, they tend to show yield stress behaviour and are commonly evaluated with use of the Herschel-Bulkley model [105], see eq. 7. Here σ_y represents the yield stress and the fitting parameters, κ, and n are the consistency and flow index, respectively. The Herschel-

Bulkley model can be modified by incorporating power law behaviour to the $\dot{\gamma}$ dependency of η [79,80], to fit more intermediate concentrations. Fits of this model have been suggested to sit in between the transition from glass (Fig. 3b) to jamming (Fig. 3d) regimes [79,83].

$$\sigma(\dot{\gamma}) = \sigma_y + \kappa\dot{\gamma}^n \tag{7}$$

The presence of σ_y implies that the system has a sufficient three dimensional network structure strong enough to at least withstand it's own weight [101], but of course the exact value of σ_y will depend on the strength of the inter- and intraparticle cross-linking and interactions.

3.2.3. Microgel architecture

As discussed above, the role of particle softness is crucial in determining the flow of microgel suspensions. The origin of the variation in the shear modulus of microgel suspensions is considered in the Evans and Lips model [106] (see Fig. 3), although this assumes that friction and adhesion forces are negligible in order to utilise descriptions of Hertzian contact mechanics. The model (eq. 8) includes a relative packing fraction, $\phi_r = \frac{\phi}{\phi_{rcp}}$, to describe ϕ in relation to ϕ_{rcp}, whilst N is the number of nearest neighbouring particles, which has been taken as $N = 10$ [74,107], although it will be dependent on the particle geometry. To implement this model, the reduced elastic modulus of the particle (E_{r_p}) must be known, which can be calculated as shown below from the Young's modulus (E_p) and Poisson's ratio (υ_p) of the particle [74]. Shewan et al. [74] used atomic force microscopy (AFM) –based nano-indentation to measure E_{r_p} of individual agarose microgels. Although measurements must consider the influence of probe type and microgel mesh size, to avoid adhesion between probe and sample [74,108,109], this appears to be the most accurate method to obtain this parameter directly.

$$G' = E_{r_p}\left[\phi_r^{\frac{1}{3}}\left(1-\phi_r^{-\frac{1}{3}}\right)^{0.5} - \left(\frac{8}{3}\right)\phi_r^{\frac{2}{3}}\left(1-\phi_r^{-\frac{1}{3}}\right)^{1.5}\right]\left(\frac{\phi_{rcp}N}{10\pi}\right) \tag{8}$$

where, $E_{r_p} = \frac{E_p}{1-\upsilon_{p^2}}$

Thus Shewan et al. [74] reported successful prediction of G' for the viscoelastic solid regime using the Evans and Lips model (Fig. 3d), with accurate prediction of an increase in G' and development of a plateau region associated with the suspension reaching a jammed state (see Fig. 3d).

Meanwhile, a polymer brush model has been used to analyse the flow behaviour of pNIPAM microgels [71,79,110]. This model considers a collection of identical polymers (i.e., a polymer brush) fixed to a solid core [110] representative of microgel interparticle interactions [71]. The derivation uses a scaling model by de Gennes [111] which incorporates the repulsion between peripheral polymer chains via a spring constant parameter [110].

To calculate the storage modulus (G'), (see eq. 9) this model focuses on the ratio between the radius of the microgel corona to its total radius via $\alpha = \frac{R_{corona}}{R_{total}}$. The volume fraction term also takes account of the divergence in rheological values at the glass transition via $\tilde{\phi} = \frac{\phi}{\phi_g}$, i.e., diverges when $\tilde{\phi}^{-\frac{1}{3}} \approx \alpha$ [79]. Across the literature, a range of α values have been reported for pNIPAM microgels, ranging from 0.49 [79] to 0.63–0.84 as the means of synthesis and cross-linker concentrations vary from 1 to 10 mol% [71,79,110].

$$G' \propto \left(\frac{1-\alpha}{\tilde{\phi}^{-\frac{1}{3}} - \alpha}\right)^{\frac{9}{4}} - \left(\frac{\tilde{\phi}^{-\frac{1}{3}} - \alpha}{1-\alpha}\right)^{\frac{3}{4}} \tag{9}$$

However, for regular synthetic microgels, this model does not hold at high concentrations where microgels have been shown to interpenetrate and G' becomes limited by the rigidity of the particle core (see Fig. 3d) rather than being dominated by the interactions of the surface dangling chains [71]. Despite this, when synthetic microgels are produced via *self*-crosslinking (i.e., those without added crosslinking agent), often reported as 'ULC' microgels, $\alpha = 0.49$ and the level of crosslinking is extremely low, giving a more regular polymer distribution and higher solvent content [79,112]. These attributes mean that the particles are thought to be freer to entangle, and subsequently their rheological behaviour has been shown to fit the brush model (eq. 9) across a wider concentration range [79] (Fig. 3). Unlike 'regular' microgels, these ULC microgels do not possess a denser core and may therefore show larger levels of interpenetration and thus the capacity for a higher effective ϕ [4,79] and the plateau in G' develops more slowly with increasing ϕ [71] and to a further extent (see Fig. 3d). Subsequently, because the area of contact and elastic forces are greater for softer particles, ϕ_{rcp} for these microgels appears to be much higher; Scotti et al. [79] reported that values of ϕ_{rcp} for 'ULC microgels' may reach >3.

It is likely that biopolymer microgels show parallels to these systems, with more loosely packed polymer chains and a higher solvent content, without a clearly defined core-corona structure, since there is less control over their formation compared to synthetic microgels. ULC architectures may be apparent within biopolymer systems and could hold great potential in terms of being able to tune the viscosity and yielding behaviour [4]. Finally, it must be noted that the behaviour of individual microgel particles in a closely packed dispersion will depend on the properties of the neighbouring particles. Compared to their synthetic counterparts, these biopolymeric microgels likely show higher levels of variation, not just in size, but also in their balance of stiffness versus the energetic costs of entanglement, which determine whether a microgel deswells (contracts) or interpenetrates with its neighbours [113]. Thus, for biopolymer systems there may be greater variation in viscoelastic and microstructural properties across the close packed solid.

3.3. Role of physiochemical factors influencing microgel rheology

As shown above in Fig. 3, physiochemical factors (temperature, ionic strength, and pH) of microgel suspensions have been considered in studies of their rheology. Below we will discuss how modification of these factors can aid in tuning microgel rheology by promoting or destroying attractive interactions.

3.3.1. Temperature

For particles of thermo-responsive synthetic polymers, the effect of temperature is via a volume phase transition, for example, the viscosity and yield strain values of pNIPAM microgel suspensions decrease as their volume phase transition temperature (VPTT) of ca. 32 °C is crossed. This is caused by an increase in hydrophobic interactions between non-polar groups and solvent release from the microgels (deswelling, see Fig. 4) which minimises particle size. Subsequently, ϕ is reduced, which aids the flow of dispersions as both electrostatic and steric interactions are minimized [77,82] and higher ϕ systems readily collapse [77,103].

For biopolymer microgels studied so far, although they do not possess a VPTT, their rheological behaviour can still vary with temperature. Some biopolymers e.g., gelatin, chitosan and cellulose possess a reversible sol-gel transition [114,115], whereby temperature variation can influence their intermolecular bonding to adjust physical cross-linking. Additionally, variations in viscosity have been reported for proteinaceous microgels when exposed to increased temperature that could be a result of changing polymer entanglements as the surface hydrophobicity of the particles is altered [75,100]. High temperatures (e.g., > 80 °C) could facilitate increased unfolding of protein chains and so promote microgel surface hydrophobicity, which may result in microgel fusion [66]. Further research could also shed insight into biopolymeric microgel behaviour at lower (refrigeration and freezing) or higher temperatures (pasteurization and sterilization) which may hold great importance in their preservation against bacterial spoilage

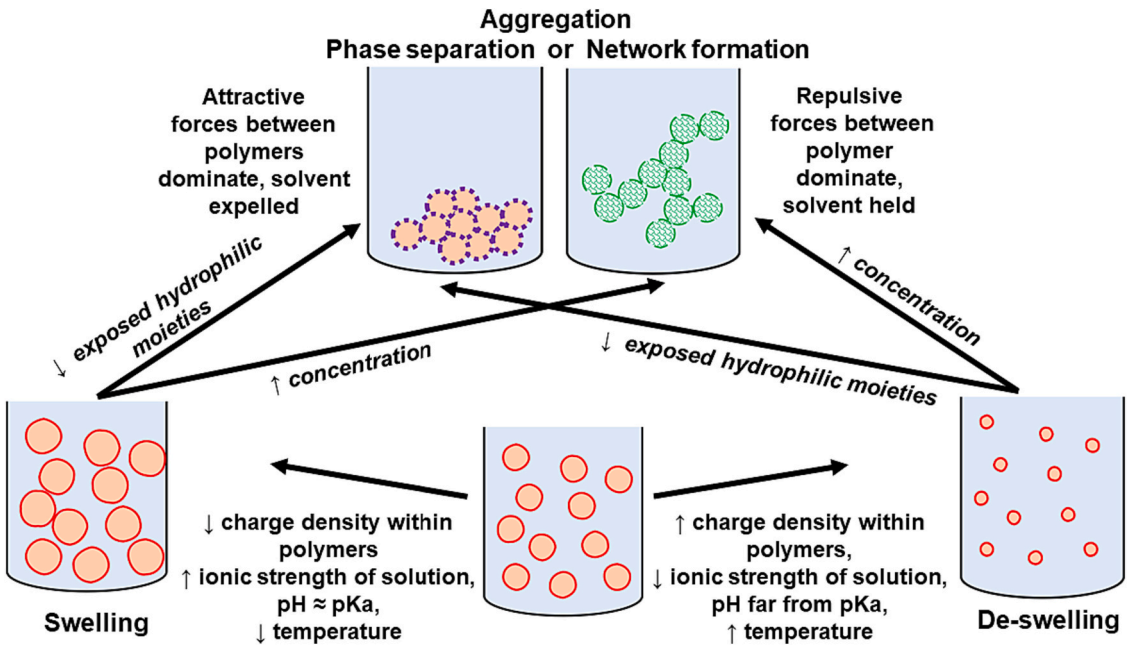

Fig. 4. Schematic illustration of fate of microgels upon exposure to environmental or processing conditions.

and processing to suit various food applications [45].

3.3.2. *Ionic strength*

The structure of the microgel dispersion also depends on the ionic strength of the system [19]. The method of synthesis or polymer used in microgel fabrication determines their charge density. Higher polymer charge density within polyacrylamide-based microgels has been shown to increase the σ_y within microgel suspensions [116]. This may be due to promotion of polymer interactions, although increased charges will tend to increase mutual repulsion between polymer chains and internally this may increase microgel rigidity that could result in a *greater* energy requirement for deformation and yielding behaviour. However, within microgels composed of methacrylic acid, internal electrostatic charges have also been proposed to lead to direct repulsions between polymer chains which promoted uptake of solvent, thus increasing swelling and microgel softness [117]. Therefore, the overall effect is likely a balance of these interactions.

The balance of polymer surface charges is also altered by salt addition [18,116]. Salt-induced aggregation of microgels can arise due to charge screening effects which can facilitate attractive polymer interactions leading to complete destabilisation and precipitation of the suspension [118]. Thus, more fluid-like properties and reductions in σ_y may be promoted due to a lack of structure, as observed for microgels originating from acrylamide, and those of pNIPAM mixtures [116,119,120] (see Fig. 4). The use of chelating agents (e.g., sodium triphosphate) has been suggested in the case of poly(acrylic acid) based microgels as a solution to avoid these effects in certain environments [121].

Aggregation has also been witnessed due to increases in temperature in systems with phosphate buffer in the aqueous phase, due to increased ionization of the phosphate [19]. Similarly, poorer solvent quality can aid network development by facilitating attractive steric interactions, *i.e.* where the outer layers have a greater tendency to stick together [32] (see Fig. 4).

3.3.3. *pH*

Charge density within microgel suspensions is also reliant on pH. For ionizable microgels, higher values of σ_y and G' have been observed for systems at pH values that promote swelling, for example for systems of polyacrylic acid this was associated with deprotonation of carboxylate groups along the polymer backbone [121]. The rheology of microgel suspensions appears to be governed by their swelling; swelling facilitates particle overlap and maximises steric interactions, which have been reported to be dominant forces in microgel interactions [32].

When interparticle charge repulsion is sufficiently strong this can promote stability and fluid-like behaviour of dispersions, but suppression of this charge can lead to colloidal gelation [18], due to stronger attractive aggregation forces between microgels (see Fig. 4). Therefore, alteration of pH in accordance with the isoelectric point of the system can enable charges to be balanced to control gelation of microgel suspensions.

In contrast, for swollen pNIPAM microgel systems *co*-polymerised with small amounts of fumaric acid, below their VPTT, their rheology was shown to be independent of ionic strength and pH [18]. Instead, this was controlled by packing levels [18] (described above), as the lower polymer density and small electrolyte content minimized the effect of surface charge repulsion [18]. Furthermore, the balance of effects between hydrophilic and hydrophobic moieties within microgels may also be varied to control particle swelling [122]. Overall, if there are few exposed hydrophilic fractions on the microgel surface, microgel swelling is inhibited and they have a greater likelihood of aggregating and expelling solvent (see Fig. 4), which may promote their aggregation.

Most biopolymers used to make microgels are polyelectrolytes and pH therefore offers the potential to alter their swelling, size, interparticle electrostatic interactions and therefore the viscosity of the suspension. This has been observed in several studies [101,104,123–125].

3.3.4. *Presence of other polymers*

Microgel interactions may also depend on their interactions with other polymers in the continuous phase, which may alter the rheology. This can lead to variations in swelling, especially when under compression or the influence of shear [76]. Whey protein microgels have been shown to behave differently in continuous phases of varying viscosity (e.g., dextran, corn syrup and low viscosity xanthan gum), disrupting interparticle interactions and modifying their rheological properties [46,76]. For example, high levels of dextran have been suggested to disrupt the flow of whey protein microgels due to promotion of steric hindrance [76], whilst the increase in viscosity reported for (low viscosity) xanthan gum upon microgel addition [46] suggests the emergence of depletion flocculation. Meanwhile, the lowering of

dispersion viscosity reported for corn syrup on the addition of microgels was suggested to arise due to drainage of buffer from the microgel particles [46] i.e. due to osmotic de-swelling.

To summarise, the prediction of microgel suspension rheology requires careful consideration of precise physiochemical parameters and is highly dependent on the system in question. Further investigation of microgel stability, particularly for biopolymeric microgels, will enable greater understanding and aid fine-tuning these systems for more controlled stability/instability on demand.

4. Microgels at interfaces

Having discussed the bulk properties of microgels, this section focuses on understanding the factors that influence the behaviour of microgels at fluid-fluid interfaces and also discusses the key tools that can be used to characterize this behaviour. Recently there have been many studies of microgel-stabilized emulsions but the details of microgel adsorption and structuring at the interface have been much more rarely addressed. As before, firstly we focus on the cleaner synthetic microgel systems then move on to compare these with biopolymeric microgels, which have been studied even less.

4.1. Synthetic microgels

Zielińska et al. [126] used neutron reflectivity to build up a picture of pNIPAM microgels at the air-water interface as comprised of three layers: a dense polymer region containing minimal water and in contact with air, a solvated polymer fraction positioned closer to the interfacial region, and finally a section of polymer chains stretching into the bulk aqueous phase. It is clear that, depending on their softness, microgels can deform on adsorption at interfaces, as evidenced in FreSCa (Freeze fracture shadow casting) cryo-SEM imaging, which has yielded images demonstrating their close packing, flattening at interfaces and protrusion into the hydrophobic phase [6,10]. However, direct visualization of microgels at interfaces is not easy due to a number of factors, such as their small size (when they are less than a few microns in diameter), the small difference in their refractive index and that of the aqueous medium, in addition to usual limitations in accurately replicating real environments during measurements. Hence imaging has often been carried out in the dried state [47,127].

Spread monolayers of microgel particles at fluid-fluid interfaces have also been studied via Langmuir troughs to analyse their response to compression [128]. In addition, once monolayers have been formed, they can then be transferred to solid substrates via Langmuir-Blodgett techniques and imaged in their dried state via microscopy techniques such as scanning electron microscopy (SEM) [129–131] and AFM [12,27,47,129–137]. This has successfully demonstrated the formation of ordered hexagonal lattice structures, which with increasing compression undergo phase transitions from corona-corona to core-core contact and then eventually monolayer collapse. Such measurements therefore provide clues to the interfacial behaviour of adsorbed microgels at increasing surface pressure.

The speed at which microgels adsorb at a fluid-fluid interface i.e., the adsorption kinetics, is dependent on a subtle balance between size, charge, hydrophobicity, and deformability [138]. Firstly, smaller size contributes to faster diffusion and enables microgels to move faster through the continuous phase to reach the interface and may influence efficiency of packing [139,140]. Meanwhile, the presence of surface-active groups on microgel surfaces allow for interaction with the interface [140,141]. Finally, deformability allows the microgel to adhere more securely to the surface: microgels continue to deform at the interface with time as the particles rearrange to develop the most desirable configuration (i.e., of lowest free energy). This may occur over long periods (e.g., hours) and is attributed to surface active groups buried within the microgel slowly becoming exposed as the particle spreads and interacts with the interface [138]. In this respect, microgel adsorption is rather similar to the adsorption and unfolding of globular proteins at an interface [142]. The extent of microgel deformation may also be influenced by solution and other external conditions, as discussed below.

4.1.1. Crosslink density and deformability

Across the literature, the amount of cross-linker incorporated into synthetic microgels varies, yet fluctuations in cross-linker values of just a few mol% (e.g., 1–5 mol%) cause significant impacts to microgel structure and their behaviour at the interface. Matsui et al. [143] directly observed microgel adsorption to a solid mica substrate via high-speed AFM and found softer pNIPAM microgels (of lower cross-linker content) to adsorb at a faster rate, which has also been corroborated by measurements of surface tension and surface pressure [138].

AFM imaging on solid substrates of more rigid microgels i.e., those of higher cross-link density, have been associated with a greater height of the microgel core [130,131,133,136,144,145] (see Fig. 5a and schematic illustration in Fig. 6). This structuring was also observed at the oil-water interface via Cryo-SEM, the microgel core protruding into the oil phase [130]. Therefore, in general, it appears that increased microgel rigidity inhibits microgel spreading at the interface [133,136] (Fig. 6). This could contribute to the formation of less stable microgel monolayers if they are unable to adapt their conformation over time or on exposure to stimuli [21]. This is further evidenced by images of microgels post Langmuir trough compression, where rigid microgels appear quicker to reach a phase transition associated with close (core-core) packing. Thus, the range and extent of compression possible for these microgels appears to be lower [131]. It has also been proposed that higher capillary attraction may occur between rigid microgels and promote closer interfacial packing and the potential for core-core interactions [131,133].

As mentioned above, some AFM studies have found that synthetic microgels display a gradient in elastic modulus, high to low, from the centre to the periphery of the particle [26,112,144–147]. However, this appears to be dependent on the concentration of cross-linker and is not always apparent: in some instances of self-crosslinked microgels (of both pNIPAM and PEG origin) the gradient in elasticity appears non-existent [146,147]. For such soft microgels that show no elasticity gradient, their structure at the interface is described as ‘disc-like’, rather than the expected ‘fried egg’ structure for regularly cross-linked synthetic microgels, and they display attributes more similar to polymer molecules at interfaces [147]. Equally, at very high concentrations of cross-linker the elasticity gradient was also reduced, as the polymer density was seen to increase across the entirety of the microgel [144]. The use of cross-linker molecules of longer length was also found to reduce values of Young’s modulus in PEG microgels (2.7–3.7 MPa was shown to fall to ca. 0.5 MPa) and has been associated with lower network density [148].

When used to stabilize emulsions, softer pNIPAM microgels appear to give greater emulsion stability, because the increased extension of their peripheral chains is thought to offer higher interfacial affinity and promote inter- and intramolecular polymer interactions, thus anchoring microgels to the interface [149]. For microgels with high levels of cross-linker, there have been reports of increased elasticity, specifically Young’s moduli, of individual microgels [144,145]. Despite this, *interfacial* rheology measurements (conducted using pendant drop tensiometry, Langmuir trough and interfacial rheology cells) have shown that for higher cross-linker levels, lower values of interfacial shear storage and loss moduli ($G_i^{'}$, $G_i^{''}$) and lower values of dilatational elasticity (ε) are seen [150]. The latter is observed by directing an oscillatory perturbation to the interface by varying the volume of a droplet, and has been utilised with microgels based on pNIPAM [150] and VCL [27]. This suggests the lack of flexibility leads to more brittle monolayers, which are more liable to fracture [150]. The authors also indicated that this correlation highlights the impact of the microgel exterior (via interactions of peripheral polymers) in dominating their interfacial

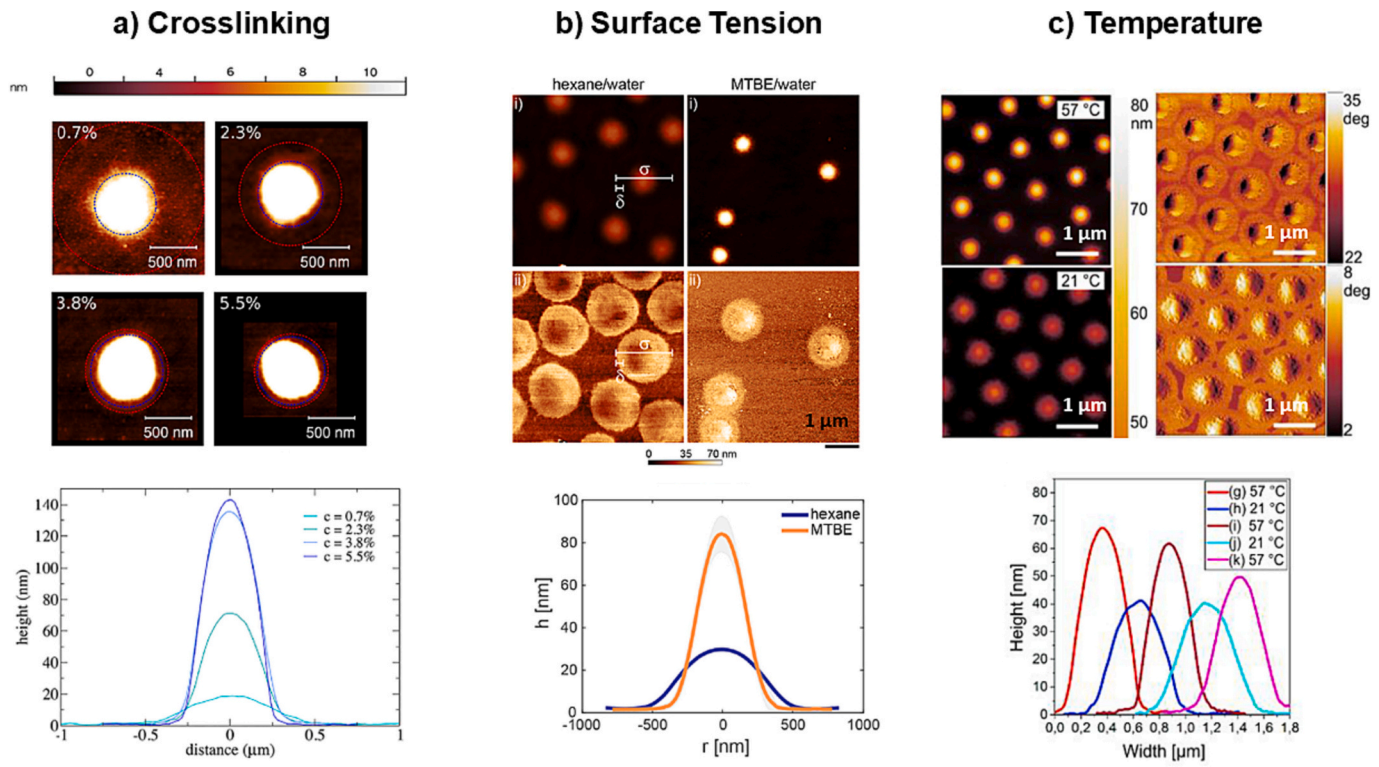

Fig. 5. Images from recent literature displaying AFM phase images (top) and AFM height measurements (bottom) in response to variations in a. crosslinking [130], b. surface tension [136] and c. temperature [129], respectively.

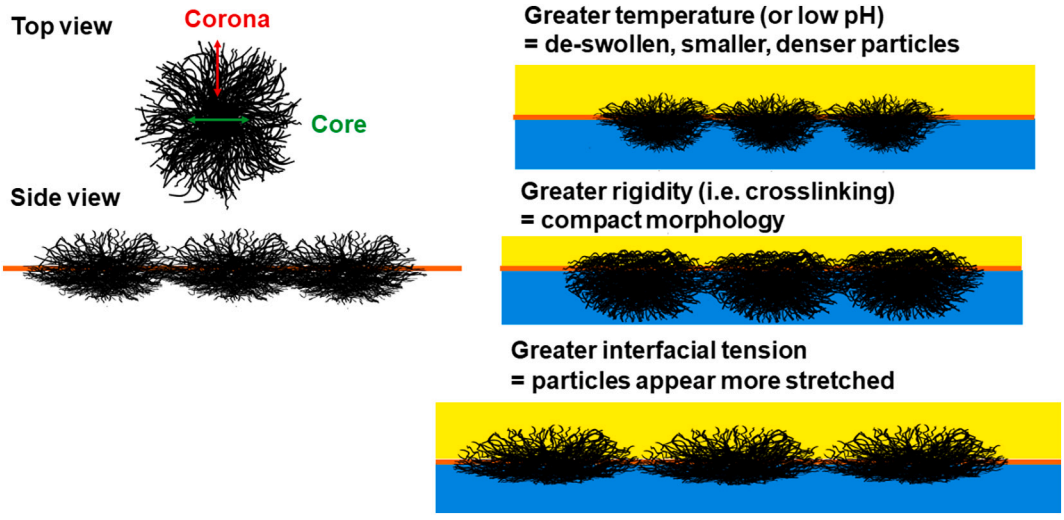

Fig. 6. Schematic displaying hypothesis of microgel interaction at oil-water interfaces.

packing behaviour [150].

For pNIPAM microgels, maxima have been reported in dilatational elastic moduli (ε') [150,151], interfacial shear moduli (G_i') [132,150,152], and elastic compression moduli (E_G) [133,150]. The first maximum has been reported at surface pressures in the range of 10 to 15 mN m^{-1}, whilst secondary peaks have also been observed at surface pressures over 30 mN m^{-1}: these are thought to correspond to shell-shell and core-core interactions, respectively [150–152]. For microgels of higher crosslinking density, E_G was in fact higher (than their softer counterparts) for the second maxima, emphasising their different morphology [150]. However, observing pNIPAM particles in shell-shell contact at the interface via cryo-SEM observations [10], Tatry et al. [150] considered that only the first maximum is of relevance to microgel stability at interfaces.

4.1.2. *Surface tension*

Due to the insolubility of pNIPAM microgels in the oil or water phases and the high values of interfacial tension, γ (72 and 50 mNm^{-1} for air-water and alkane-water interfaces at 25 °C, respectively) [136] microgel deformation has been observed at the interface. Deformation arises to minimise interfacial free energy, as shown below in eq. 10, the change in interfacial free energy (ΔG) for spherical colloidal particles can be calculated based on γ, radius of the particle (R) and the contact angle (θ) [153]. Although, microgel particles cannot be directly

compared to Pickering systems of rigid particles, these parameters still largely influence microgel adsorption and associated "Mickering stabilization" [5].

$$\Delta G = -\pi R^2 \gamma [1 - cos(\theta)]^2 \quad (10)$$

For alternative non-alkane oils, in addition to their potential to act as solvents for pNIPAM microgels [47,154], γ may be lower and therefore modify microgel adsorption [136]. For example, methyl tert-butyl ether (MTBE) (interfacial tension of 9.8 mNm^{-1}) yielded observations [136], of higher values of core height but smaller overall diameters of microgels, when compared to alkane-water interfaces (see Fig. 5a). Stiffer monolayers were also reported for microgels adsorbing at interfaces with higher γ, compared to those at lower γ which were seen to collapse more readily when compressed [136]. Similar behaviour has been reported for microgel adsorption to solid surfaces of varying surface hydrophobicity. For example, STORM was used to observe poly(N-isopropylmethacrylamide) (pNIPMAM) microgels at glass surfaces of varying hydrophilicity [155]. This demonstrated the alteration of the adsorbed microgel configuration from completely spread to only partially wetted, which resulted in a change of appearance from the flattened 'fried-egg'-like structure to a near-spherical configuration [155].

Microgels stretch across interfaces to minimise the undesirable contact between the repulsive hydrophilic and hydrophobic phases, so that at the interfaces of different phases possessing different γ, the extent of this deformation can be altered. Hence low values of γ appear to limit microgel spreading at the interface, allowing for the elasticity of microgel polymers to determine the final extent of deformation at the interface [6]. This is probably particularly relevant for microgel adsorption at water-water interfaces, where γ is extremely low [104,156].

Effects of microgel size may also be responsible for apparent discrepancies in variations in the extent of deformation with respect to γ. Bochenek et al. [47] studied microgels of size (d_H at 20 °C) 300 nm and observed them to flatten to a greater level at an air-water interface compared to a decane-water interface. This difference in deformation was not reported in similar investigations [129,130,136] with microgels of more than twice the size. It was hypothesised that beyond a certain γ (ca. 36 mN m^{-1}) a maximum in pNIPAM microgel extension was reached [130,136].

4.1.3. Electrostatics

For pNIPAM microgels, anionic charges are usually introduced via the co-monomers (e.g. methacrylic acid (MAA) or acrylic acid (AA)) or the initiator potassium peroxodisulfate (KPS) [117,135], and show electrophoretic mobility (at room temperature) in the range of −2 to $-2.5 \times 10^{-8}\ m^2\ V^{-1}\ s^{-1}$ compared to values of almost zero obtained for uncharged samples [133,135,157]. AFM topographic imaging has shown that high charge density and pH of methacrylic acid microgels can alter their water content and thus their levels of flattening at interfaces [117]. For charged microgels that have also shrunk due to temperatures above the VPTT, further compression reaches a limit whereby electrostatic repulsion between the particles leads to their desorption [157]. Overall, it can be seen that, like their behaviour in bulk solution, the interfacial behaviour of microgels is determined by their level of swelling and is a result of combined environmental conditions and nature of the polymer itself in controlling the moieties which may be available to interact.

Nonetheless, there has been controversy within the literature on the role of electrostatics (i.e., ionic strength and pH variation) in stimulating deformation of both charged or near neutral microgels at interfaces. Picard et al. [133] stated that variation in electrostatics had no observable impact on microgel deformation, but this observation may be associated with their use of pNIPAM microgels of size ca. 600 nm diameter and the specific pH range 3 to 6. Meanwhile, Kwok and Ngai [158] observed anisotropic flattening of pNIPAM microgel particles on decane oil in water droplets via confocal microscopy, although this deformation was only seen at high pH (pH 10). The authors proposed that pNIPAM microgels that are not fully swollen may undergo lower levels of interfacial deformation [158]. Meanwhile, Yang et al. [157] suggested that charged microgels were more sensitive to compression, whereas Schmidt et al. [135] found that at higher levels of compression, uncharged microgels showed greater compressibility. It was proposed that this latter trend was due to the positioning of the microgel: whether a greater area was either in-plane or perpendicular to the interface [135]. Charged microgels were found to have a greater area of their particle out of plane due to a higher level of interaction with the aqueous phase (due to their higher levels of swelling), contributing to their greater compressibility at low compression levels. Therefore, it was suggested that the influence of low compression was determined by in-plane interactions, whereas high compression was thought to be reliant on out of plane interactions. This variation in compressibility with charge was also thought to be dependent on size, since the phenomenon was not observed in larger microgel particles (ca. 850 nm diameter) [135].

4.1.4. Temperature

As described above, thermo-responsive pNIPAM microgels have a VPTT above which an increase of hydrophobic interactions causes solvent expulsion [27]. In this shrunken state, the peripheral dangling chains of the microgel are thought to collapse onto the inner core, decreasing their size [129] (see Figs. 5 and 6). However, microgels have been shown to maintain their interfacial activity even when collapsed at higher temperatures [140].

AFM nanoindentation methods have provided lateral mapping of microgels, giving an elastic modulus across individual microgel particles deposited on a solid substrate within a fluid environment [26,109,144,147,159,160]. The stiffness of the microgels increases at temperatures above VPTT and a loss of long-range repulsion between the AFM probe and microgel has been observed in force-distance curves, linked to a reduction in steric forces after the collapse of dangling polymer chains [161]. Furthermore, AFM imaging has shown a decrease in microgel height and diameter as solvent leaves the microgel structure and the particles become denser and less deformable [160,162] (see Figs. 5c and 6).

Harrer et al. [129] also used AFM phase contrast imaging to show that the area of the corona of pNIPAM microgels is independent of temperature. It was proposed that the lower water content and stretched nature of the corona region at the interface led to a greater influence of γ and that this dominated the positioning of the microgel particles overall at the interface [129]. Bochenek et al. [134] supported this finding via ellipsometry, determining the microgel region within aqueous solution as exclusively thermo-responsive. Consequently, this portion of the microgel de-swells, decreasing the monolayer thickness and core diameter above the VPTT. It was implied by both studies [129,134] that, due to the corona's relative lack of sensitivity towards temperature, the spacing and extent of microgel coverage at the interface was constant throughout temperature variations [129,134] (see Fig. 5c). Additionally, studies of regular and ULC pNIPAM microgels via neutron reflectivity demonstrated that the behaviour of the microgel portions protruding into the air were independent of temperature fluctuations [163].

Despite the numerous reports of *destabilisation* of pNIPAM microgel-stabilized emulsions above VPTT [164], Tatry et al. [21] reported a study of poly(oligoethylene glycol) methacrylate (pOEMA) microgel-stabilized emulsions that did not phase separate above the VPTT. They hypothesised that although some coalescence is likely to have occurred, the softness of the microgels may have facilitated compression and lateral interpenetration, which created an optimal level of cohesion allowing adjustment of microgel configurations that avoided complete destabilisation [21]. Overall, the above studies reiterate the importance

of understanding microgel deformability with respect to stabilization of emulsions by microgels at the interface.

4.2. Biopolymeric microgels

To finalise, the behaviour of biopolymeric microgels at interfaces is now discussed. Although there are much fewer studies of these systems, differences are starting to emerge between biopolymeric and synthetic microgels as described below.

Confocal microscopy (see Figs. 7a-c) has been widely utilised to obtain images of thick layers of microgels at oil-water interfaces. The regular packing and uniform morphology of adsorbed layers of synthetic pNIPAM microgels is not apparent for biopolymeric systems. This can also be observed in cryo-SEM images (see Figs. 7d-f).

Deformation of biopolymeric microgels has been successfully observed using cryo-SEM (see Table 1) at both oil-water and air-water interfaces [44,45,124,166,167] and greater deformability is generally correlated with greater interfacial stability. Meanwhile, AFM has helped to illustrate aggregation [168–170], polydispersity [171], and the presence of smaller (likely surface-active) components within biopolymeric microgel monolayers [169,170]. Compared to the regular, domed structure of synthetic microgels (e.g., as in Fig. 7g), AFM observations of biopolymeric microgels have shown the presence of small clusters (Fig. 7h) [46]. Such clusters might develop into larger aggregates during monolayer compression and have a detrimental impact on interfacial stability having been proposed to trigger the collapse of microgel monolayers [170].

Microgel aggregation may be triggered by electrostatic interactions [171–173], but low microgel surface coverage has also been proposed as a possible cause in both synthetic and biopolymeric microgels due to dominance of capillary forces [152,168]. Murphy et al. [168] suggested that greater surface loading of microgel particles could also prevent emulsion droplet aggregation, implying that steric hindrance may be a determining factor in maintaining stability. Flocculation of emulsion droplets may also occur at higher microgel particle concentrations [174], although this may not necessarily have a detrimental impact, since the aggregates can still adhere to interfaces but also bridge between droplets [175]. Furthermore, microgel aggregation could facilitate the formation of microgel multilayers on the droplets, which may further promote the mechanical strength of the microgel film [176].

Similar to synthetic microgels, the imaging of biopolymeric monolayers has also been conducted via AFM: several studies have recently visualised monolayers formed after compression with the use of a Langmuir trough in combination with AFM [168,170] whilst the surface formed during QCM-D measurements has also been visualised [173]. Table 1 shows articles from 2016 onwards which have explored the interfacial behaviour of biopolymeric microgels. The table highlights the range of methodologies used in their fabrication, in addition to the relatively few papers that have used a range of characterization techniques to understand their surface properties. The findings from these studies are discussed below.

4.2.1. Surface activity

Across the majority of studies listed in Table 1, interfacial tension (γ) measurement was found to be a key characterization tool to assess interfacial behaviour. As described previously for synthetic microgels, biopolymeric microgels also rely on hydrophobic groups to interact with and adsorb to an interface. Depending on biopolymer type, sufficient hydrophobic groups may not be available at the microgel particle surface [174]. For example, pectin, agar, gellan gum and curdlan microgels have all been studied via pendant drop tensiometry [167,174]. Typically, a significant reduction in γ is observed in protein-based microgels, which reflects the microgels' adsorption kinetics. However, such reduction of γ is not seen in the polysaccharide-based microgels due to lack of hydrophobic moieties [167,174]. Further analyses beyond measurements of surface activity often appear necessary to gain understanding of the origin of microgel interfacial stability.

It is thought that biopolymeric microgel particles also unfold and rearrange at interfaces to develop the lowest energy configuration, which generally involves maximal exposure of hydrophobic groups to

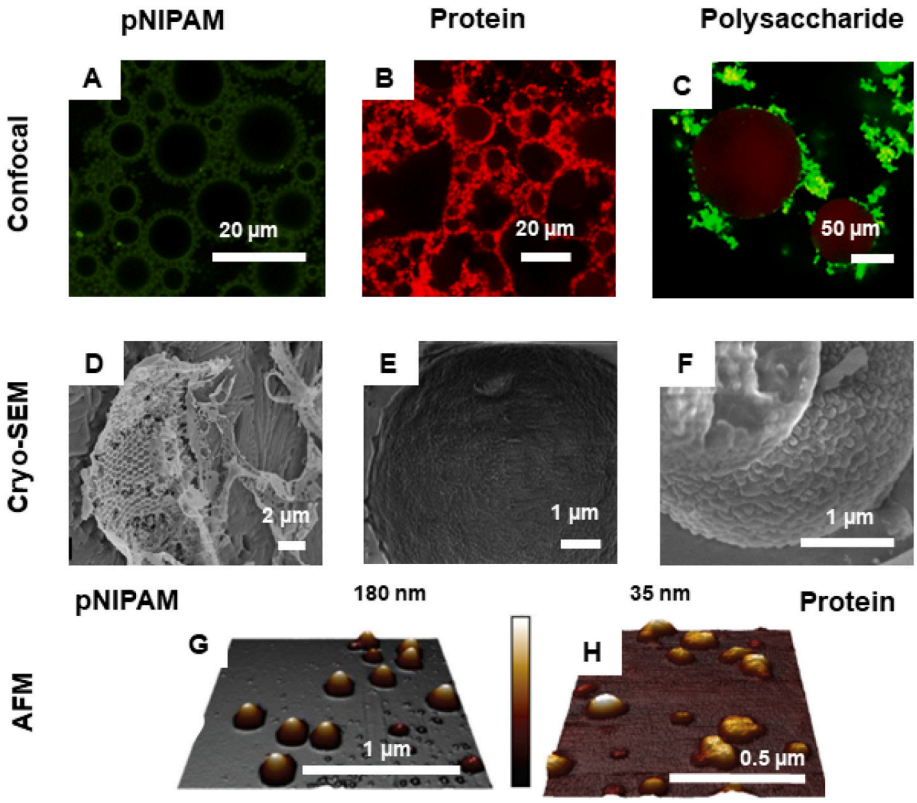

Fig. 7. Micrographs of protein and pNIPAM microgels obtained using various techniques. Top row: Confocal microscopy of A) pNIPAM microgel [158], B) Whey protein microgel [165] and C) Chitosan microgel [125], all at oil-water interface. Middle row: Cyro-SEM images of oil-water emulsion droplets stabilized by D) pNIPAM microgels with 0.05 M NaCl [138], E) Genipen crosslinked casein protein microgels [166], and F) Curdlan microgels [167]. Bottom row: AFM imaging in contact mode of G) pNIPAM microgel [144] and H) Whey protein microgel [46] both hydrated on silicon wafer solid substrate.

the non-aqueous phase and thus an increase in interfacial coverage [3,141]. Despite this, particle rigidity may limit unfolding and thus inhibit surface activity [177]. Huang et al. [125] reported slower adsorption of highly swollen microgel particles which was linked to an adsorption barrier arising from increased repulsive steric interactions. Although microgel swelling to some extent may aid in adsorption it has been proposed that deformation of softer microgels creates a larger wetting radius, which could promote a stronger capillary attraction to the interface [176]. Chen et al. [176] observed whey protein microgels of varying protein content via ellipsometry and found that those of lowest biopolymer content have a greater adsorption capacity, which facilitated the formation of a thicker interfacial layer. Surface adsorption may also be altered by variations in particle size and charge, since larger microgels diffuse more slowly, whilst increased microgel charge (such as that originating from pH values ≠ pI) can contribute to an electrostatic adsorption barrier [173,177]. Additionally, it has been suggested that at high concentrations microgel diffusion is slowed due to increased viscosity [172].

In some cases (see Table 1), the three-phase contact angle of microgels has been evaluated to determine their hydrophobicity (see eq. 10 above). However, the relevance of this measurement is debatable as microgel particles, particularly those of biopolymeric origin, do not necessarily hold a fixed shape, plus they are porous to the phases at the interface [3,141]. Through modifications to production methods, biopolymeric microgels with contact angles close to 90^0 have been observed [172,177,178]. These contact angles were correlated with greater wettability and interfacial stability than native biopolymers, whilst also being linked to a decline in interfacial rearrangement [177,178].

Considering the potential benefit of microgel flexibility at the interface in producing resilient monolayers, this correlation could appear contradictory to the previous discussion. Despite this, these studies suggested that due to their near optimal contact angle (i.e., 90^0) the microgel would not be required to rearrange its configuration [177,178].

4.2.2. Surface coverage and conformation

As shown in Table 1, the investigation of microgel elasticity can be conducted using several techniques. Interfacial measurements of dilatational and shear rheology can aid in evaluating the viscoelasticity of the interfacial microgel layer, whilst increasingly AFM is being utilised to analyse the nanomechanical properties of individual biopolymeric microgels. This has allowed for stiffness values to be calculated [125], whilst more commonly values of Young's modulus are obtained [171,176].

Li et al. [45] studied the interfacial shear viscosity (η_i) of egg white protein microgels at the air-water interface. Despite observations of a slower development of η_i compared to native protein, they reported much higher η_i ($> 10^4$ mN s m^{-1}) for the microgels after 1400 min compared to non-microgelled protein. This again suggests that the larger size of the microgels slows their initial binding to the interface, yet at greater timescales it appears that their superior coverage (cf. native protein) may enable the development of an optimal configuration [45]. It was suggested that the adsorbed microgel layer displayed more resilience compared to the native protein, as the latter displayed a drop in viscosity at longer times [45].

Meanwhile, Yang et al. [169] studied an interfacial layer formed of whey protein isolate 'beads', via oscillatory dilatational and surface shear rheology, yet found conversely that these beads gave a lower interfacial shear moduli ($G_i^{'}$, $G_i^{''}$) (by over 2 orders of magnitude) compared to native whey protein and whey protein aggregates. They concluded that the 'beads' formed a weaker, more mobile layer, which relied on the small components of the suspension to stabilize the interface [169]. The true extent of microgels' influence on interfaces has been debated by numerous authors who consider smaller surface-active components to also have a role in interfacial stability (e.g., free protein, protein or microgel fragments that remain in the microgel suspension or trapped by the microgel) [170,179]. Ultrafiltration was suggested to have removed unbound protein from microgel dispersions such that the resultant microgel samples showed an increasingly slower development of surface pressure and plateaus at values of >5 mN m^{-1} lower, highlighting the potential role of smaller surface-active constituents [179]. Meanwhile, Noskov et al. [170] purified their beta-lactoglobulin microgel suspensions and reported increases in interfacial dilatational elasticity (ε) which were associated with an increase in intra-particle interactions. However, regardless of purification it was shown that microgels had an increased ε when compared to native protein.

In contrast, for soy protein microgels lower values of dilatational modulus have been found (cf. native protein) and attributed to weaker intermolecular forces and the formation of a more rigid configuration [177]. This result may be specific to the biopolymer type or production method, see Table 1, if these factors reduced polymer hydrophobicity to an extent which limited inter- and/or intra-particle interactions. Meanwhile, investigation of beta-lactoglobulin microgels suggested that the tighter packing of smaller microgels may decrease values of ε [168], highlighting the additional role of size in creating an interfacial layer of optimal mobility.

Further comparisons of whey protein microgels (see Table 1) of varying rigidity showed that the most deformable microgels studied, (5 wt% protein content), displayed the highest values of dilatational elastic and viscous moduli ($\varepsilon_i^{'}$, $\varepsilon_i^{''}$) [176]. However, it was noted that this study of micron-sized microgels appeared to yield values of ε lower than those found in studies of microgels of smaller, nanometer size. Despite this, deformability may aid in promoting the adsorption of hydrophobic binding sites to the interface since with greater mobility the configuration of microgels has a greater capacity to adapt [125,176]. It was found that use of softer microgel stabilisers led to emulsions with greater stability, whilst the more rigid are likely to lead to fragile interfacial layers [125,176].

4.2.3. Electrostatics

Modification of pH has been shown to alter the size of whey protein microgels, by triggering biopolymer rearrangement via electrostatic repulsion and increased protein chain stress at pH values ≠ pI [171]. Subsequently, AFM imaging and force spectroscopy, demonstrated a reduction in microgel flattening and an increase in values of Young's modulus calculated at the centre of microgels [171] in acidic conditions. Moreover, Huang et al. [125] investigated the ε of chitosan microgels in response to varying pH finding that pH values which facilitated microgel swelling and thus softer microgels led to higher ε (up to 60 mN m^{-1} for microgels at pH 4). These values were also significantly higher than those observed for the native polysaccharide, hence the study concluded that microgels of highest deformation were able to laterally overlap to create a stabilising network at interfaces [125].

The influence of pH and ionic strength were also analysed with the use of QCM-D [173]. At pH values further from the pI of whey protein microgels (pH 3.2, 7.4) microgels were more strongly charged and less surface coverage was observed, whilst at pH 5.6 a highly covered interface was reported. FTIR analysis implied that conformational changes occurred for whey protein microgels at pH 3.2 which may have aided in their interfacial coverage compared to looser structures observed at pH 7.4 [173]. Meanwhile, an increase in ionic strength facilitated closer, denser packing of microgels due to shielding of electrostatic repulsion, which led to reportedly increased rigidity at the interface [173]. Furthermore, addition of K^+ to κ-carrageenan microgels has been reported to increase their hardness and this was suggested to increase their viscoelasticity, although at the highest levels tested (250 mM) shrinkage of microgels was discovered which led to aggregation and destruction of their stabilising ability [172].

5. Conclusions and future perspectives

This review has given a comprehensive examination of experimental and theoretical aspects of bulk and interfacial properties of microgels. Recent literature is increasingly investigating the impact of the extent of microgel interaction in bulk solution at high volume fractions, where densely packed 'jammed' systems display unique properties (e.g., microgel interpenetration, faceting) which offer novel ways to alter the viscosity of continuum. Meanwhile, interfacial systems of microgels are also becoming a greater area of research focus for control of emulsion stability. We derive some commonalities between synthetic and biopolymeric microgels, including:

- Both microgel types show rheological behaviour (in η_r, G') that deviates from hard sphere models, in particular at volume fractions beyond 0.4-0.5, as microgel particles begin to interact and the capacity for dense microgel packing increases.
- Microgels show interfacial activity modulated by the balance of the surface tension of the system and the elasticity of the individual particles which can be adapted by altering the polymer and system (e.g., emulsion) type, plus the means of microgel fabrication.
- Both forms of microgel possess the capacity to de-swell and swell when subjected to varying physiochemical conditions offering the potential for controlled de-stabilization within bulk and at interfaces.
- Regardless of their nature, the elasticity of microgels appears to display a pivotal role in maintaining both their interfacial stability and ability for viscosity modification by facilitating inter-particle interactions whilst altering particle configurations to minimize the free energy.

Nevertheless, there are some differences between synthetic and biopolymeric microgels, including:

- Generally, biopolymeric microgels are more polydisperse whilst synthetic microgels are more likely to be monodisperse, since polymerisation allows for control via precise use chemical crosslinking agents.
- At interfaces, the presence of non-microgel species may contribute to surface activity for biopolymeric microgels. This is less prevalent for synthetic microgels because their chemical synthesis again allows for greater control.
- Aggregation appears to pose a significant influence on microgel monolayer stability for biopolymeric systems; this could lead to randomly distributed areas of high polymer density that promote destabilisation.
- The apparent lack of a core-corona structure [170] could mean biopolymeric microgels have a different method of interfacial stabilization to synthetic microgels. Furthermore, this suggests that biopolymer microgels are more loosely crosslinked, which could facilitate the development of higher ϕ (greater levels of packing) within dispersions and a more gradual development of bulk viscosity as microgels may be able to interpenetrate to a greater extent.
- Biopolymeric microgels are produced from inherently complex, naturally occurring proteins and polysaccharides, sometimes their mixtures that vary in charge distribution, chain lengths, hydrophobic groups etc. and threfore the structure and properties are not as controllable as monodisperse synthetic microgels even in lab settings.

Overall, optimal conditions for surface coverage and responsiveness will vary depending on the system in question, yet the preservation of microgel mobility at the interface appears to be imperative in promoting their performance as stabilisers and ensuring that they can adjust their configuration to provide resilient packing. The extent of microgel interpenetration within bulk and at interfaces is not fully understood for biopolymeric particles, therefore, the role of inter-particle interaction in their stabilising ability is still an important question to be answered in fully understanding the mechanism of microgel packing. This would also facilitate our understanding in optimisation of biopolymeric microgel performance to ensure that microgels are effective emulsifiers whilst meeting the demands for economic viability, batch to batch reproducibility and utilisation of appropriate isolation methods (of biopolymer) [29].

This review highlights the need for more comprehensive characterization of microgel systems (in particular those of biopolymeric origin) to include a broader range of techniques to accurately deduce microgel packing in their native state (i.e., in fluid, at fluid-fluid interfaces) at the nanoscale. Furthermore, systematic and comparative investigations of biopolymeric microgel systems produced from different biopolymer sources are required to shed light on the impact of environmental factors as well as their variabilities (i.e., size, polydispersity, and moduli) on interfacial performance. Due to the difficulty in visualising these particles at fluid interfaces precisely without altering their form, greater information acquired from different sources of characterization such as combining monolayer experiments with in situ visualization of the surface layer using AFM, would allow for increased justification of current hypotheses on microgel interfacial and bulk performance. Finally, the literature disproportionately focuses on animal protein-based microgels, particularly whey protein microgels, for the biopolymeric systems. With environmental sustainability challenges, it will be imperative to characterize the bulk and interfacial properties of microgels from alternative proteins such as plant proteins and microorganism-derived biopolymeric sources to enable design of the next generation of sustainable microgels for various soft matter and allied applications.

Declaration of Competing Interest

Authors declare no conflicts of interests. The views expressed in this manuscript are those of the authors and do not necessarily reflect the position or policy of PepsiCo, Inc.

Data availability

No data was used for the research described in the article.

Acknowledgements

Authors gratefully acknowledge the Engineering and Physical Sciences Research Council (EPSRC) funded Centre for Doctoral Training in Soft Matter for Formulation and Industrial Innovation (SOFI2), Grant Ref. No. EP/S023631/1 for financial support. This work was co-funded by PepsiCo, Inc. The views expressed in this manuscript are those of the authors and do not necessarily reflect the position or policy of PepsiCo, Inc.

References

[1] Scheffold F. Pathways and challenges towards a complete characterization of microgels. Nat Commun 2020;11:4315.
[2] Lima CSA, Balogh TS, Varca J, Varca GHC, Lugao AB, L AC-C, et al. An Updated Review of Macro, Micro, and Nanostructured Hydrogels for Biomedical and Pharmaceutical Applications Pharmaceutics. 2020. p. 12.
[3] Dickinson E. Microgels — an alternative colloidal ingredient for stabilization of food emulsions. Trends Food Sci Technol 2015;43:178–88.
[4] Scotti A, Schulte MF, Lopez CG, Crassous JJ, Bochenek S, Richtering W. How softness matters in soft nanogels and nanogel assemblies. Chem Rev 2022;122:11675–700.
[5] Schmidt S, Liu T, Rutten S, Phan KH, Moller M, Richtering W. Influence of microgel architecture and oil polarity on stabilization of emulsions by stimuli-sensitive core-shell poly(N-isopropylacrylamide-co-methacrylic acid) microgels: Mickering versus Pickering behavior? Langmuir. 2011;27:9801–6.
[6] Fernandez-Rodriguez MA, Martin-Molina A, Maldonado-Valderrama J. Microgels at interfaces, from mickering emulsions to flat interfaces and back. Adv Colloid Interface Sci 2021;288:18.

[7] Stock S, von Klitzing R. Microgels at droplet interfaces of water-in-oil emulsions—challenges and progress. Curr Opin Colloid Interface Sci 2022;58.
[8] Ciarella S, Rey M, Harrer J, Holstein N, Ickler M, Lowen H, et al. Soft particles at liquid interfaces: from molecular particle architecture to collective phase behavior. Langmuir. 2021;37:5364–75.
[9] Kolker J, Harrer J, Ciarella S, Rey M, Ickler M, Janssen LMC, et al. Interface-induced hysteretic volume phase transition of microgels: simulation and experiment. Soft Matter 2021;17:5581–9.
[10] Destribats M, Lapeyre V, Wolfs M, Sellier E, Leal-Calderon F, Ravaine V, et al. Soft microgels as Pickering emulsion stabilisers: role of particle deformability. Soft Matter 2011;7.
[11] Pelton RH, Chibante P. Preparation of aqueous latices with N-isopropylacrylamide. Colloids Surf 1986;20:247–56.
[12] Scheidegger L, Fernandez-Rodriguez MA, Geisel K, Zanini M, Elnathan R, Richtering W, et al. Compression and deposition of microgel monolayers from fluid interfaces: particle size effects on interface microstructure and nanolithography. Phys Chem Chem Phys 2017;19:8671–80.
[13] Shin DS, Tokuda EY, Leight JL, Miksch CE, Brown TE, Anseth KS. Synthesis of microgel sensors for spatial and temporal monitoring of protease activity. ACS Biomater Sci Eng 2018;4:378–87.
[14] Goudarzi A, Almohsin A, Varavei A, Taksaudom P, Hosseini SA, Delshad M, et al. New laboratory study and transport model implementation of microgels for conformance and mobility control purposes. Fuel. 2017;192:158–68.
[15] Johann S, Weichert FG, Schroer L, Stratemann L, Kampfer C, Seiler TB, et al. A plea for the integration of green toxicology in sustainable bioeconomy strategies - biosurfactants and microgel-based pesticide release systems as examples. J Hazard Mater 2022;426:127800.
[16] Shanmugam S, Ross G, Mbuncha CY, Santra A. Rapid, green synthesis of high performance viscosifiers via a photoiniferter approach for water-based drilling fluids. Polym Chem 2021;12:6705–13.
[17] Kılıç S. Forty years of NAD microgels as rheology control agents. Prog Org Coat 2016;98:35–8.
[18] Minami S, Yamamoto A, Oura S, Watanabe T, Suzuki D, Urayama K. Criteria for colloidal gelation of thermo-sensitive poly(N-isopropylacrylamide) based microgels. J Colloid Interface Sci 2020;568:165–75.
[19] Town A, Niezabitowska E, Kavanagh J, Barrow M, Kearns VR, Garcia-Tunon E, et al. Understanding the phase and morphological behavior of dispersions of synergistic dual-stimuli-responsive poly(N-isopropylacrylamide) nanogels. J Phys Chem B 2019;123:6303–13.
[20] Tatry MC, Qiu Y, Lapeyre V, Garrigue P, Schmitt V, Ravaine V. Sugar-responsive Pickering emulsions mediated by switching hydrophobicity in microgels. J Colloid Interface Sci 2020;561:481–93.
[21] Tatry MC, Galanopoulo P, Waldmann L, Lapeyre V, Garrigue P, Schmitt V, et al. Pickering emulsions stabilized by thermoresponsive oligo(ethylene glycol)-based microgels: effect of temperature-sensitivity on emulsion stability. J Colloid Interface Sci 2021;589:96–109.
[22] Chen Z, Feng Y, Zhao N, Liu Y, Liu G, Zhou F, et al. Near-infrared-light-modulated lubricating coating enabled by photothermal microgels. ACS Appl Mater Interfaces 2021;13:49322–30.
[23] Jelken J, Jung SH, Lomadze N, Gordievskaya YD, Kramarenko EY, Pich A, et al. Tuning the volume phase transition temperature of microgels by light. Adv Funct Mater 2021;32.
[24] Maity S, Mishra B, Nayak K, Dubey NC, Tripathi BP. Zwitterionic microgel based anti(−bio)fouling smart membranes for tunable water filtration and molecular separation. Mater Today Chem 2022:24.
[25] Yogev S, Shabtay-Orbach A, Nyska A, Mizrahi B. Local toxicity of topically administrated Thermoresponsive systems: in vitro studies with in vivo correlation. Toxicol Pathol 2019;47:426–32.
[26] Wilms D, Adler Y, Schroer F, Bunnemann L, Schmidt S. Elastic modulus distribution in poly(N-isopopylacrylamide) and oligo(ethylene glycol methacrylate)-based microgels studied by AFM. Soft Matter 2021;17:5711–7.
[27] Maldonado-Valderrama J, del Castillo-Santaella T, Adroher-Benitez I, Moncho-Jorda A, Martin-Molina A. Thermoresponsive microgels at the air-water interface: the impact of the swelling state on interfacial conformation. Soft Matter 2017;13:230–8.
[28] Tafuro G, Costantini A, Baratto G, Francescato S, Semenzato A. Evaluating natural alternatives to synthetic acrylic polymers: rheological and texture analyses of polymeric water dispersions. ACS Omega 2020;5:15280–9.
[29] McClements DJ, Gumus CE. Natural emulsifiers - biosurfactants, phospholipids, biopolymers, and colloidal particles: molecular and physicochemical basis of functional performance. Adv Colloid Interface Sci 2016;234:3–26.
[30] Baranwal J, Barse B, Fais A, Delogu GL, Kumar A. Biopolymer: a sustainable material for food and medical applications. Polymers (Basel) 2022:14.
[31] Shewan HM, Stokes JR. Review of techniques to manufacture micro-hydrogel particles for the food industry and their applications. J Food Eng 2013;119:781–92.
[32] McClements DJ. Designing biopolymer microgels to encapsulate, protect and deliver bioactive components: physicochemical aspects. Adv Colloid Interface Sci 2017;240:31–59.
[33] Wechsler ME, Stephenson RE, Murphy AC, Oldenkamp HF, Singh A, Peppas NA. Engineered microscale hydrogels for drug delivery, cell therapy, and sequencing. Biomed Microdevices 2019;21:31.
[34] Torres O, Murray B, Sarkar A. Emulsion microgel particles: novel encapsulation strategy for lipophilic molecules. Trends Food Sci Technol 2016;55:98–108.
[35] Torres O, Tena NM, Murray B, Sarkar A. Novel starch based emulsion gels and emulsion microgel particles: design, structure and rheology. Carbohydr Polym 2017;178:86–94.
[36] Torres O, Murray B, Sarkar A. Design of novel emulsion microgel particles of tuneable size. Food Hydrocoll 2017;71:47–59.
[37] Torres O, Andablo-Reyes E, Murray BS, Sarkar A. Emulsion microgel particles as high-performance bio-lubricants. ACS Appl Mater Interfaces 2018;10:26893–905.
[38] Zeeb B. Interaction between components of plant-based biopolymer systems. Curr Opin Colloid Interface Sci 2021;56.
[39] Sadasivuni KK, Saha P, Adhikari J, Deshmukh K, Ahamed MB, Cabibihan JJ. Recent advances in mechanical properties of biopolymer composites: a review. Polym Compos 2019;41:32–59.
[40] Garcia-Moreno PJ, Gregersen S, Nedamani ER, Olsen TH, Marcatili P, Overgaard MT, et al. Identification of emulsifier potato peptides by bioinformatics: application to omega-3 delivery emulsions and release from potato industry side streams. Sci Rep 2020;10:690.
[41] Haldar D, Shabbirahmed AM, Singhania RR, Chen CW, Dong CD, Ponnusamy VK, et al. Understanding the management of household food waste and its engineering for sustainable valorization- a state-of-the-art review. Bioresour Technol 2022;358:127390.
[42] Sarkar A, Dickinson E. Sustainable food-grade Pickering emulsions stabilized by plant-based particles. Curr Opin Colloid Interface Sci 2020;49:69–81.
[43] Zhang S, Holmes M, Ettelaie R, Sarkar A. Pea protein microgel particles as Pickering stabilisers of oil-in-water emulsions: Responsiveness to pH and ionic strength. Food Hydrocoll 2020:102.
[44] Destribats M, Rouvet M, Gehin-Delval C, Schmitt C, Binks BP. Emulsions stabilised by whey protein microgel particles: towards food-grade Pickering emulsions. Soft Matter 2014;10:6941–54.
[45] Li X, Murray BS, Yang Y, Sarkar A. Egg white protein microgels as aqueous Pickering foam stabilizers: Bubble stability and interfacial properties. Food Hydrocoll 2020:98.
[46] Andablo-Reyes E, Yerani D, Fu M, Liamas E, Connell S, Torres O, et al. Microgels as viscosity modifiers influence lubrication performance of continuum. Soft Matter 2019;15:9614–24.
[47] Bochenek S, Scotti A, Richtering W. Temperature-sensitive soft microgels at interfaces: air-water versus oil-water. Soft Matter 2021;17:976–88.
[48] Fernandez-Nieves A. Microgel suspensions : Fundamentals and applications. Weinheim, Germany: Wiley-VCH; 2011.
[49] Murray BS. Microgels at fluid-fluid interfaces for food and drinks. Adv Colloid Interface Sci 2019;271:101990.
[50] Cutright CC, Harris JL, Ramesh S, Khan SA, Genzer J, Menegatti S. Surface-bound microgels for separation, sensing, and biomedical applications. Adv Funct Mater 2021;31.
[51] Dave R, Randhawa G, Kim D, Simpson M, Hoare T. Microgels and nanogels for the delivery of poorly water-soluble drugs. Mol Pharm 2022;19:1704–21.
[52] Papagiannopoulos A, Sotiropoulos K. Current advances of polysaccharide-based nanogels and microgels in food and biomedical sciences. Polymers (Basel) 2022;14.
[53] Mehrabian H, Harting J, Snoeijer JH. Soft particles at a fluid interface. Soft Matter 2016;12:1062–73.
[54] Mehrabian H, Snoeijer JH, Harting J. Desorption energy of soft particles from a fluid interface. Soft Matter 2020;16:8655–66.
[55] Gumerov RA, Rudyak VY, Gavrilov AA, Chertovich AV, Potemkin II. Effect of network topology and crosslinker reactivity on microgel structure and ordering at liquid-liquid interface. Soft Matter 2022;18:3738–47.
[56] Staudinger H, Husemann E. Über hochpolymere Verbindungen, 116. Mitteil.: Über das begrenzt quellbare Poly-styrol. Berichte der deutschen chemischen Gesellschaft (A and B Series)68; 1935. p. 1618–34.
[57] Baker WO. Microgel, a new macromolecule. Ind Eng Chem 1949;41:511–20.
[58] Sieglaff CL. Viscosity and swelling behaviour of lightly crosslinked microgels. Polymer. 1963;4:281–4.
[59] Taylor NW, Bagley EB. Dispersions or solutions? A mechanism for certain thickening agents. J Appl Polym Sci 1974;18:2747–61.
[60] Bartsch E, Kirsch S, Lindner P, Scherer T, Stölken S. Spherical microgel colloids — hard spheres from soft matter. Ber Bunsen Phys Chem 1998;102:1597–602.
[61] Zhang J, Pelton R. Poly(N-isopropylacrylamide) microgels at the air−water Interface. Langmuir. 1999;15:8032–6.
[62] Lynn DM, Amiji MM, Langer R. pH-responsive polymer microspheres: rapid release of encapsulated material within the range of intracellular pH. Angew Chem-Int Edit 2001;40:1707–10.
[63] Ngai T, Behrens SH, Auweter H. Novel emulsions stabilized by pH and temperature sensitive microgels. Chem Commun (Camb) 2005;331-3.
[64] Schmitt C, Bovay C, Vuilliomenet AM, Rouvet M, Bovetto L, Barbar R, et al. Multiscale characterization of individualized beta-lactoglobulin microgels formed upon heat treatment under narrow pH range conditions. Langmuir. 2009;25:7899–909.
[65] Brown AC, Stabenfeldt SE, Ahn B, Hannan RT, Dhada KS, Herman ES, et al. Ultrasoft microgels displaying emergent platelet-like behaviours. Nat Mater 2014;13:1108–14.
[66] Sarkar A, Murray B, Holmes M, Ettelaie R, Abdalla A, Yang XY. In vitro digestion of Pickering emulsions stabilized by soft whey protein microgel particles: influence of thermal treatment. Soft Matter 2016;12:3558–69.
[67] Wang C, Geng Y, Sun Q, Xu J, Lu Y. A sustainable and efficient artificial microgel system: toward creating a configurable synthetic cell. Small. 2020;16:e2002313.

[68] Switacz VK, Wypysek SK, Degen R, Crassous JJ, Spehr M, Richtering W. Influence of size and cross-linking density of microgels on cellular uptake and uptake kinetics. Biomacromolecules. 2020;21:4532–44.
[69] Bouhid de Aguiar I, van de Laar T, Meireles M, Bouchoux A, Sprakel J, Schroen K. Deswelling and deformation of microgels in concentrated packings. Sci Rep 2017; 7:10223.
[70] Conley GM, Aebischer P, Nojd S, Schurtenberger P, Scheffold F. Jamming and overpacking fuzzy microgels: deformation, interpenetration, and compression. Sci Adv 2017;3:7.
[71] Conley GM, Zhang C, Aebischer P, Harden JL, Scheffold F. Relationship between rheology and structure of interpenetrating, deforming and compressing microgels. Nat Commun 2019;10:2436.
[72] Franco S, Buratti E, Ruzicka B, Nigro V, Zoratto N, Matricardi P, et al. Volume fraction determination of microgel composed of interpenetrating polymer networks of PNIPAM and polyacrylic acid. J Phys-Condes Matter 2021;33:12.
[73] Scotti A. Characterization of the volume fraction of soft deformable microgels by means of small-angle neutron scattering with contrast variation. Soft Matter 2021;17:5548–59.
[74] Shewan HM, Yakubov GE, Bonilla MR, Stokes JR. Viscoelasticity of non-colloidal hydrogel particle suspensions at the liquid-solid transition. Soft Matter 2021;17: 5073–83.
[75] Sarkar A, Kanti F, Gulotta A, Murray BS, Zhang SY. Aqueous lubrication, structure and rheological properties of whey protein microgel particles. Langmuir. 2017; 33:14699–708.
[76] Soltanahmadi S, Murray BS, Sarkar A. Comparison of oral tribological performance of proteinaceous microgel systems with protein-polysaccharide combinations. Food Hydrocoll 2022;129.
[77] Chaudhary G, Ghosh A, Kang JG, Braun PV, Ewoldt RH, Schweizer KS. Linear and nonlinear viscoelasticity of concentrated thermoresponsive microgel suspensions. J Colloid Interface Sci 2021;601:886–98.
[78] Ghosh A, Chaudhary G, Kang JG, Braun PV, Ewoldt RH, Schweizer KS. Linear and nonlinear rheology and structural relaxation in dense glassy and jammed soft repulsive pNIPAM microgel suspensions. Soft Matter 2019;15:1038–52.
[79] Scotti A, Brugnoni M, Lopez CG, Bochenek S, Crassous JJ, Richtering W. Flow properties reveal the particle-to-polymer transition of ultra-low crosslinked microgels. Soft Matter 2020;16:668–78.
[80] Pellet C, Cloitre M. The glass and jamming transitions of soft polyelectrolyte microgel suspensions. Soft Matter 2016;12:3710–20.
[81] Bhattacharjee T, Kabb CP, O'Bryan CS, Uruena JM, Sumerlin BS, Sawyer WG, et al. Polyelectrolyte scaling laws for microgel yielding near jamming. Soft Matter 2018;14:1559–70.
[82] Dieuzy E, Aguirre G, Auguste S, Chougrani K, Alard V, Billon L, et al. Microstructure-driven self-assembly and rheological properties of multi-responsive soft microgel suspensions. J Colloid Interface Sci 2021;581:806–15.
[83] Franco S, Buratti E, Nigro V, Zaccarelli E, Ruzicka B, Angelini R. Glass and jamming rheology in soft particles made of PNIPAM and polyacrylic acid. Int J Mol Sci 2021;22:17.
[84] Stubley SJ, Cayre OJ, Murray BS, Celigueta Torres I. Pectin-based microgels for rheological modification in the dilute to concentrated regimes. J Colloid Interface Sci 2022;628:684–95.
[85] Rudyak VY, Sergeev AV, Kozhunova EY, Molchanov VS, Philippova OE, Chertovich AV. Viscosity of macromolecules with complex architecture. Polymer. 2022;244.
[86] Khalil N, de Candia A, Fierro A, Ciamarra MP, Coniglio A. Dynamical arrest: interplay of glass and gel transitions. Soft Matter 2014;10:4800–5.
[87] Minami S, Watanabe T, Suzuki D, Urayama K. Rheological properties of suspensions of thermo-responsive poly(N-isopropylacrylamide) microgels undergoing volume phase transition. Polym J 2016;48:1079–86.
[88] Ikeda A, Berthier L, Sollich P. Disentangling glass and jamming physics in the rheology of soft materials. Soft Matter 2013;9.
[89] Agarwal M, Kaushal M, Joshi YM. Signatures of overaging in an aqueous dispersion of carbopol. Langmuir. 2020;36:14849–63.
[90] Shewan HM, Stokes JR. Viscosity of soft spherical micro-hydrogel suspensions. J Colloid Interface Sci 2015;442:75–81.
[91] Roullet M, Clegg PS, Frith WJ. Viscosity of protein-stabilized emulsions: contributions of components and development of a semipredictive model. J Rheol 2019;63:179–90.
[92] Batchelor GK. The effect of Brownian motion on the bulk stress in a suspension of spherical particles. J Fluid Mech 1977;83:97–117.
[93] Bicerano J, Douglas JF, Brune DA. Model for the viscosity of particle dispersions. J Macromol Sci Part C 1999;39:561–642.
[94] Einstein A. A new determination of the molecular dimensions. Ann Phys 1906;19: 289–306.
[95] Mueller S, Llewellin EW, Mader HM. The rheology of suspensions of solid particles. Proc Roy Soc A Math Phys Eng Sci 2009;466:1201–28.
[96] Quemada D. Rheology of concentrated disperse systems and minimum energy dissipation principle. Rheol Acta 1977;16:82–94.
[97] Krieger IM, Dougherty TJ. A mechanism for non-Newtonian flow in suspensions of rigid spheres. Trans Soc Rheol 1959;3:137–52.
[98] Farr RS, Groot RD. Close packing density of polydisperse hard spheres. J Chem Phys 2009;131:244104.
[99] Shamana H, Grossutti M, Papp-Szabo E, Miki C, Dutcher JR. Unusual polysaccharide rheology of aqueous dispersions of soft phytoglycogen nanoparticles. Soft Matter 2018;14:6496–505.
[100] Zembyla M, Lazidis A, Murray BS, Sarkar A. Stability of water-in-oil emulsions co-stabilized by polyphenol crystal-protein complexes as a function of shear rate and temperature. J Food Eng 2020;281:9.
[101] Olivares ML, Achkar NP, Zorrilla SE. Rheological behavior of concentrated skim milk dispersions as affected by physicochemical conditions: change in pH and CaCl2 addition. Dairy Sci Technol 2016;96:525–38.
[102] Stubley SJ, Cayre OJ, Murray BS, Torres IC, Farrés IF. Enzyme cross-linked pectin microgel particles for use in foods. Food Hydrocoll 2021;121.
[103] Sbeih S, Mohanty PS, Morrow MR, Yethiraj A. Structural parameters of soft PNIPAM microgel particles as a function of crosslink density. J Colloid Interface Sci 2019;552:781–93.
[104] Murray BS, Phisarnchananan N. Whey protein microgel particles as stabilizers of waxy corn starch plus locust bean gum water-in-water emulsions. Food Hydrocoll 2016;56:161–9.
[105] Herschel WH, Bulkley R. Konsistenzmessungen von Gummi-Benzollösungen Kolloid-Zeitschrift39; 1926. p. 291–300.
[106] Evans ID, Lips A. Concentration dependence of the linear elastic behaviour of model microgel dispersions. J Chem Soc Faraday Trans 1990;86:3413–7.
[107] Rognon PG, Einav I, Gay C. Flowing resistance and dilatancy of dense suspensions: lubrication and repulsion. J Fluid Mech 2011;689:75–96.
[108] Bonilla MR, Stokes JR, Gidley MJ, Yakubov GE. Interpreting atomic force microscopy nanoindentation of hierarchical biological materials using multi-regime analysis. Soft Matter 2015;11:1281–92.
[109] Schulte MF, Izak-Nau E, Braun S, Pich A, Richtering W, Gostl R. Microgels react to force: mechanical properties, syntheses, and force-activated functions. Chem Soc Rev 2022;51:2939–56.
[110] Scheffold F, Diaz-Leyva P, Reufer M, Ben Braham N, Lynch I, Harden JL. Brushlike interactions between thermoresponsive microgel particles. Phys Rev Lett 2010; 104:128304.
[111] de Gennes PG. Conformations of polymers attached to an Interface. Macromolecules. 1980;13:1069–75.
[112] Scotti A, Bochenek S, Brugnoni M, Fernandez-Rodriguez MA, Schulte MF, Houston JE, et al. Exploring the colloid-to-polymer transition for ultra-low crosslinked microgels from three to two dimensions. Nat Commun 2019;10:1418.
[113] Scotti A, Denton AR, Brugnoni M, Houston JE, Schweins R, Potemkin II, et al. Deswelling of microgels in crowded suspensions depends on cross-link density and architecture. Macromolecules. 2019;52:3995–4007.
[114] Xu Y, Qi R, Zhu H, Li B, Shen Y, Krainer G, et al. Liquid-liquid phase-separated systems from reversible gel-sol transition of protein microgels. Adv Mater 2021; 33:e2008670.
[115] Chatterjee S, Hui PC. Review of applications and future prospects of stimuli-responsive hydrogel based on thermo-responsive biopolymers in drug delivery systems. Polymers (Basel) 2021:13.
[116] O'Bryan CS, Kabb CP, Sumerlin BS, Angelini TE. Jammed polyelectrolyte microgels for 3D cell culture applications: rheological behavior with added salts. ACS Appl Bio Mater 2019;2:1509–17.
[117] Nystrom L, Alvarez-Asencio R, Frenning G, Saunders BR, Rutland MW, Malmsten M. Electrostatic swelling transitions in surface-bound microgels. ACS Appl Mater Interfaces 2016;8:27129–39.
[118] Minami S, Suzuki D, Urayama K. Rheological aspects of colloidal gels in thermoresponsive microgel suspensions: formation, structure, and linear and nonlinear viscoelasticity. Curr Opin Colloid Interface Sci 2019;43:113–24.
[119] Wang T, Jin L, Song YN, Li JX, Gao Y, Shi S. Rheological study on the thermoinduced gelation behavior of poly(N-isopropylacrylamide-co-acrylic acid) microgel suspensions. J Appl Polym Sci 2017;134:8.
[120] Wang T, Jin L, Zhang Y, Song YN, Li JX, Gao Y, et al. In situ gelation behavior of thermoresponsive poly(N-vinylpyrrolidone)/poly(N-isopropylacrylamide) microgels synthesized by soap-free emulsion polymerization. Polym Bull 2018;75: 4485–98.
[121] Shafiei M, Bryant S, Balhoff M, Huh C, Bonnecaze RT. Hydrogel formulation for sealing cracked wellbores for Co2 storage. Appl Rheol (Lappersdorf, Germany) 2017;27:27–34.
[122] Arzumand A, Srinivas S, Yuan Y, Zhou C, Sarkar D. Mechano-morphological characterization of polyethylene-glycol based polyurethane microgel. Macromol Mater Eng 2016;301:1158–71.
[123] Li XM, Wu ZZ, Zhang B, Pan Y, Meng R, Chen HQ. Fabrication of chitosan hydrochloride and carboxymethyl starch complex nanogels as potential delivery vehicles for curcumin. Food Chem 2019;293:197–203.
[124] İnce Coşkun AE, Özdestan Ocak Ö. Foaming behavior of colloidal whey protein isolate micro-particle dispersions. Colloids Surf A Physicochem Eng Asp 2021; 609.
[125] Huang P, Huang C, Ma X, Gao C, Sun F, Yang N, et al. Effect of pH on the mechanical, interfacial, and emulsification properties of chitosan microgels. Food Hydrocoll 2021;121.
[126] Zielinska K, Sun H, Campbell RA, Zarbakhsh A, Resmini M. Smart nanogels at the air/water interface: structural studies by neutron reflectivity. Nanoscale. 2016;8: 4951–60.
[127] Nishizawa Y, Honda K, Suzuki D. Recent development in the visualization of microgels. Chem Lett 2021;50:1226–35.
[128] Gong Y, Zhang ZL, He JY. Deformation and stability of Core-Shell microgels at oil/water Interface. Ind Eng Chem Res 2017;56:14793–8.
[129] Harrer J, Rey M, Ciarella S, Lowen H, Janssen LMC, Vogel N. Stimuli-responsive behavior of PNiPAm microgels under interfacial confinement. Langmuir. 2019; 35:10512–21.

[130] Camerin F, Fernandez-Rodriguez MA, Rovigatti L, Antonopoulou MN, Gnan N, Ninarello A, et al. Microgels adsorbed at liquid-liquid interfaces: a joint numerical and experimental study. ACS Nano 2019;13:4548–59.
[131] Rey M, Hou XA, Tang JSJ, Vogel N. Interfacial arrangement and phase transitions of PNiPAm microgels with different crosslinking densities. Soft Matter 2017;13:8717–27.
[132] Rey M, Fernandez-Rodriguez MA, Steinacher M, Scheidegger L, Geisel K, Richtering W, et al. Isostructural solid-solid phase transition in monolayers of soft core-shell particles at fluid interfaces: structure and mechanics. Soft Matter 2016;12:3545–57.
[133] Picard C, Garrigue P, Tatry MC, Lapeyre V, Ravaine S, Schmitt V, et al. Organization of microgels at the air-water interface under compression: role of electrostatics and cross-linking density. Langmuir. 2017;33:7968–81.
[134] Bochenek S, Scotti A, Ogieglo W, Fernandez-Rodriguez MA, Schulte MF, Gumerov RA, et al. Effect of the 3D swelling of microgels on their 2D phase behavior at the liquid-liquid Interface. Langmuir. 2019;35:16780–92.
[135] Schmidt MM, Bochenek S, Gavrilov AA, Potemkin II, Richtering W. Influence of charges on the behavior of polyelectrolyte microgels confined to oil-water interfaces. Langmuir. 2020;36:11079–93.
[136] Vialetto J, Nussbaum N, Bergfreund J, Fischer P, Isa L. Influence of the interfacial tension on the microstructural and mechanical properties of microgels at fluid interfaces. J Colloid Interface Sci 2022;608:2584–92.
[137] Sasaki Y, Hiroshige S, Takizawa M, Nishizawa Y, Uchihashi T, Minato H, et al. Non-close-packed arrangement of soft elastomer microspheres on solid substrates. RSC Adv 2021;11:14562–7.
[138] Tatry MC, Laurichesse E, Perro A, Ravaine V, Schmitt V. Kinetics of spontaneous microgels adsorption and stabilization of emulsions produced using microfluidics. J Colloid Interface Sci 2019;548:1–11.
[139] Maestro A, Jones D, de Rojas Sanchez, Candela C, Guzman E, Duits MHG, et al. Tuning interfacial properties and processes by controlling the rheology and structure of poly(N-isopropylacrylamide) particles at air/water interfaces. Langmuir. 2018;34:7067–76.
[140] Dan A, Agnihotri P, Bochenek S, Richtering W. Adsorption dynamics of thermoresponsive microgels with incorporated short oligo(ethylene glycol) chains at the oil-water interface. Soft Matter 2021;17:6127–39.
[141] Murray BS. Microgels at fluid-fluid interfaces for food and drinks. Adv Colloid Interface Sci 2019;271:7.
[142] Murray BS, Ettelaie R, Sarkar A, Mackie AR, Dickinson E. The perfect hydrocolloid stabilizer: imagination versus reality. Food Hydrocoll 2021;117:19.
[143] Matsui S, Kureha T, Hiroshige S, Shibata M, Uchihashi T, Suzuki D. Fast adsorption of soft hydrogel microspheres on solid surfaces in aqueous solution. Angew Chem Int Ed Engl 2017;56:12146–9.
[144] Aufderhorst-Roberts A, Baker D, Foster RJ, Cayre O, Mattsson J, Connell SD. Nanoscale mechanics of microgel particles. Nanoscale 2018;10:16050–61.
[145] Mohapatra H, Kruger TM, Lansakara TI, Tivanski AV, Stevens LL. Core and surface microgel mechanics are differentially sensitive to alternative crosslinking concentrations. Soft Matter 2017;13:5684–95.
[146] Welsch N, Lyon LA. Oligo(ethylene glycol)-sidechain microgels prepared in absence of cross-linking agent: polymerization, characterization and variation of particle deformability. PLoS One 2017;12:e0181369.
[147] Schulte MF, Bochenek S, Brugnoni M, Scotti A, Mourran A, Richtering W. Stiffness tomography of ultra-soft nanogels by atomic force microscopy. Angew Chem Int Ed Engl 2021;60:2280–7.
[148] Schroer F, Paul TJ, Wilms D, Saatkamp TH, Jack N, Muller J, et al. Lectin and E. coli binding to carbohydrate-functionalized oligo(ethylene glycol)-based microgels: effect of elastic modulus, crosslinker and carbohydrate density. Molecules. 2021:26.
[149] Kwok MH, Ngai T. Comparing the relative interfacial affinity of soft colloids with different crosslinking densities in Pickering emulsions. Front Chem 2018;6:12.
[150] Tatry MC, Laurichesse E, Vermant J, Ravaine V, Schmitt V. Interfacial rheology of model water-air microgels laden interfaces: effect of cross-linking. J Colloid Interface Sci 2022;629:288–99.
[151] Akentiev AV, Rybnikova GS, Novikova AA, Timoshen KA, Zorin IM, Noskov BA. Dynamic elasticity of films formed by poly(N-isopropylacrylamide) microparticles on a water surface. Colloid J 2017;79:571–6.
[152] Huang SL, Gawlitza K, von Klitzing R, Steffen W, Auernhammeer GK. Structure and rheology of microgel monolayers at the water/oil Interface. Macromolecules. 2017;50:3680–9.
[153] Maestro A. Tailoring the interfacial assembly of colloidal particles by engineering the mechanical properties of the interface. Curr Opin Colloid Interface Sci 2019;39:232–50.
[154] Rumyantsev AM, Gumerov RA, Potemkin II. A polymer microgel at a liquid-liquid interface: theory vs. computer simulations. Soft Matter 2016;12:6799–811.
[155] Hoppe Alvarez L, Eisold S, Gumerov RA, Strauch M, Rudov AA, Lenssen P, et al. Deformation of microgels at solid-liquid interfaces visualized in three-dimension. Nano Lett 2019;19:8862–7.
[156] Murray BS, Ettelaie R. Chapter 5: Bijel systems based on the phase separation of biological macromolecules. In: RSC Soft Matter; 2020. p. 114–36. 2020-January.
[157] Yang Y, Maldonado-Valderrama J, Martin-Molina A. Temperature and electrostatics effects on charged poly(N-isopropylacrylamide) microgels at the interface. J Mol Liq 2020;303:8.
[158] Kwok MH, Ngai T. A confocal microscopy study of micron-sized poly (N-isopropylacrylamide) microgel particles at the oil-water interface and anisotopic flattening of highly swollen microgel. J Colloid Interface Sci 2016;461:409–18.
[159] Witte J, Kyrey T, Lutzki J, Dahl AM, Kühnhammer M, Rv Klitzing, et al. Looking inside poly(N-isopropylacrylamide) microgels: nanomechanics and dynamics at solid–liquid interfaces. ACS Appl Polym Mater 2021;3:976–85.
[160] Li G, Varga I, Kardos A, Dobryden I, Claesson PM. Temperature-dependent nanomechanical properties of adsorbed poly-NIPAm microgel particles immersed in water. Langmuir. 2021;37:1902–12.
[161] Bochenek S, McNamee CE, Kappl M, Butt HJ, Richtering W. Interactions between a responsive microgel monolayer and a rigid colloid: from soft to hard interfaces. Phys Chem Chem Phys 2021;23:16754–66.
[162] Liu M, Chen XL, Yang ZP, Xu Z, Hong LZ, Ngai T. Tunable Pickering emulsions with environmentally responsive hairy silica nanoparticles. ACS Appl Mater Interfaces 2016;8:32250–8.
[163] Bochenek S, Camerin F, Zaccarelli E, Maestro A, Schmidt MM, Richtering W, et al. In-situ study of the impact of temperature and architecture on the interfacial structure of microgels. Nat Commun 2022;13:3744.
[164] Rey M, Uttinger MJ, Peukert W, Walter J, Vogel N. Probing particle heteroaggregation using analytical centrifugation. Soft Matter 2020;16:3407–15.
[165] Chu Y, Wismer W, Zeng H, Chen L. Contribution of protein microgels, protein molecules, and polysaccharides to the emulsifying behaviors of core/shell whey protein-alginate microgel systems. Food Hydrocoll 2022;129.
[166] Wang P, Chen C, Guo H, Zhang H, Yang Z, Ren F. Casein gel particles as novel soft Pickering stabilizers: the emulsifying property and packing behaviour at the oil-water interface. Food Hydrocoll 2018;77:689–98.
[167] Ishii T, Matsumiya K, Aoshima M, Matsumura Y. Microgelation imparts emulsifying ability to surface-inactive polysaccharides-bottom-up vs top-down approaches. NPJ Sci Food 2018;2:15.
[168] Murphy RW, Farkas BE, Jones OG. Dynamic and viscoelastic interfacial behavior of beta-lactoglobulin microgels of varying sizes at fluid interfaces. J Colloid Interface Sci 2016;466:12–9.
[169] Yang J, Thielen I, Berton-Carabin CC, van der Linden E, Sagis LMC. Nonlinear interfacial rheology and atomic force microscopy of air-water interfaces stabilized by whey protein beads and their constituents. Food Hydrocoll 2020;101:10.
[170] Noskov BA, Rafikova AR, Yu. Milyaeva O.. β-Lactoglobulin microgel layers at the surface of aqueous solutions. J Mol Liq 2022:351.
[171] Bahri A, Chevalier-Lucia D, Marchesseau S, Schmitt C, Gergely C, Martin M. Effect of pH change on size and nanomechanical behavior of whey protein microgels. J Colloid Interface Sci 2019;555:558–68.
[172] Jiang QB, Li SY, Du LY, Liu YF, Meng Z. Soft kappa-carrageenan microgels stabilized Pickering emulsion gels: compact interfacial layer construction and particle-dominated emulsion gelation. J Colloid Interface Sci 2021;602:822–33.
[173] Zhang JL, Mei L, Chen NN, Yuan Y, Zeng QZ, Wang Q. Study on beta-lactoglobulin microgels adsorption onto a hydrophobic solid surface by QCM-D. Food Hydrocoll 2020;98:10.
[174] Isusi GIS, Bindereif B, Karbstein HP, van der Schaaf US. Polymer or microgel particle: differences in emulsifying properties of pectin as microgel or as individual polymer chains. Coll Surf A-Physicochem Eng Asp 2020;598:9.
[175] Zembyla M, Lazidis A, Murray BS, Sarkar A. Water-in-oil Pickering emulsions stabilized by synergistic particle-particle interactions. Langmuir. 2019;35:13078–89.
[176] Chen S, Du Y, Zhang H, Wang Q, Gong Y, Chang R, et al. The lipid digestion behavior of oil-in-water Pickering emulsions stabilized by whey protein microgels of various rigidities. Food Hydrocoll 2022;130.
[177] Guo J, Zhou Q, Liu YC, Yang XQ, Wang JM, Yin SW, et al. Preparation of soy protein-based microgel particles using a hydrogel homogenizing strategy and their interfacial properties. Food Hydrocoll 2016;58:324–34.
[178] Sun Y, Ma L, Fu Y, Dai H, Zhang Y. Fabrication and characterization of myofibrillar microgel particles as novel Pickering stabilizers: Effect of particle size and wettability on emulsifying capacity. Lwt 2021;151.
[179] Silva JTD, Nicoletti VR, Schroen K, de Ruiter J. Enhanced coalescence stability of droplets through multi-faceted microgel adsorption behaviour. J Food Eng 2022;317:10.